Review

Optical tweezers for single cells

Hu Zhang and Kuo-Kang Liu*

Institute for Science and Technology in Medicine, Keele University,
Stoke-on-Trent ST4 7QB, UK

Optical tweezers (OT) have emerged as an essential tool for manipulating single biological cells and performing sophisticated biophysical/biomechanical characterizations. Distinct advantages of using tweezers for these characterizations include non-contact force for cell manipulation, force resolution as accurate as 100 aN and amiability to liquid medium environments. Their wide range of applications, such as transporting foreign materials into single cells, delivering cells to specific locations and sorting cells in microfluidic systems, are reviewed in this article. Recent developments of OT for nanomechanical characterization of various biological cells are discussed in terms of both their theoretical and experimental advancements. The future trends of employing OT in single cells, especially in stem cell delivery, tissue engineering and regenerative medicine, are prospected. More importantly, current limitations and future challenges of OT for these new paradigms are also highlighted in this review.

Keywords: optical tweezers; micromanipulation; microfluidic devices; cell sorting; cellular biomechanics; tissue engineering

1. INTRODUCTION

Manipulating single cells is of paramount importance in areas of biomedical research such as *in vitro* fertilization, cell–cell interaction, cell adhesion, embryology, microbiology, stem cell, tissue engineering and regenerative medicine and single cell transfection. The examination of how individual cells operate, function and interact with each other can reveal invisible processes such as single cell gene expression and chemical communication inside a singe cell, and can elucidate connections between subcellular processes and population-level behaviour. Two major types of techniques have been developed for manipulation of single cells: one is scanning probes such as the atomic force microscope (AFM) and scanning tunnel microscope (STM) and the other is field gradient traps such as optical tweezers (OT), magnetic tweezers (MT) and dielectrophoretic (DEP) traps. The working principles, merits and demerits of those techniques are summarized in table 1.

OT have been widely applied to single molecular and cellular studies. At a single molecular level, biological motors including kinesin (Asbury *et al.* 2003; Block *et al.* 2003), cytoplasmic dynein (Mallik *et al.* 2004), myosin (Knight *et al.* 2001; Swank *et al.* 2001), nucleic acid-based enzymes (Pease *et al.* 2005; Dumont *et al.* 2006) and flagellar motors (Ryu *et al.* 2000) have been extensively studied as well as RNA and DNA mechanics

(Allemand *et al.* 2003; Bustamante *et al.* 2003), protein conformational changes in folding/unfolding pathway (Cecconi *et al.* 2005), protein–protein binding/unbinding process (Thoumine *et al.* 2000; Litvinov *et al.* 2005) and DNA–protein interaction (Williams *et al.* 2001; Huisstede *et al.* 2007). Comprehensive reviews have been made for the OT: physical theory of optical trapping (Ashkin 1997, 2007), microsurgery (Berns 1998) and biophysical analysis of single molecules (Hormeno & Arias-Gonzalez 2006). A summary concerning the theory, construction and applications of OT can be found in Sheetz (1998), Ashkin (2007) and Berns & Greulich (2007).

In this review, the focus is mainly on how to apply OT for manipulating single cells and their mechanical characterization. Various cell types, including mammalian cells, *Escherichia coli*, red blood cells (RBCs), nerve cells, gametes and stem cells, have been studied. Modelling of cell mechanics and cell deformation in optical trapping is also appraised. Finally, future trends of OT for single cells, especially stem cells for tissue engineering and regenerative medicines, are prospected.

2. WORKING PRINCIPLES

2.1. Trapping mechanisms

OT use a highly focused laser beam to trap and manipulate microscopic, neutral objects such as small dielectric spherical particles that experience two kinds

*Author for correspondence (i.k.liu@keele.ac.uk).

Table 1. Comparison of common micromanipulation tools for single cells[a]. (AFM, atomic force microscopy; MT, magnetic tweezers; DEP, dielectrophoresis; OT, optical tweezers.)

tools		principle	type	length-scale probe (nm)	typical force range (pN)	stiffness (pN nm^{-1})	advantages	disadvantages
scanning probes	AFM	a sharp tip normal to the free end of a cantilever	point; contact	1–10 000	5–10 000	10–10 000	active force clamp	single cell needs to adhere tightly to a surface; random attachment
field gradient traps	MT	electromagnetic field gradients; magnetic beads that are attached to single cell surface	global/point; non-contact	10–10 000	0.05–20	10^{-6}– 0.1	constant force; angular force for out-of-plane rotation of single cell	magnetic beads to covalent or specific non-covalent attached to cells
	DEP	high-gradient electric field; cell dielectric properties and the surrounding medium	global; non-contact	20–100 000	0.01–50	—	simple operation	heating; two-dimensional trap
	OT	A highly focused beam to produce optical gradient; cell refraction index	point; non-contact	0.1–1000	0.1–100	10^{-6}– 0.1	non-contact force; active or passive force clamp; well-defined geometries	photodamage or thermal damage

[a] Some data are cited from Greenleaf *et al.* (2007).

of forces as explained in figure 1*a*, namely the scattering force produced by the photons striking the cell along their propagation direction and the gradient force produced by a gradient of field intensity. Scattering and gradient forces exerted on the particles depend on the wavelength of the laser beam (λ) and the particle size (r). Particles trapped by the OT can be divided into three regimes: Mie regime ($r \gg \lambda$); Rayleigh regime ($r \ll \lambda$); and regime in between them ($r \sim \lambda$) (Ashkin & Dziedzic 1987; Ashkin 2007).

In the Mie regime, where the particle size is larger than the wavelength of the irradiation light, both the magnitude and the direction of the forces depend on the particle shape and trapping is generally restricted to spheres and ellipsoids. The conservation of momentum model or ray optics is applicable to this case (Ashkin 1997). Any change of momentum from individual rays of light when striking the particle results in an equal, opposite momentum change on the particle. A more intensive beam imparts a larger momentum change towards the centre of the trap than the less intensive beam. As shown in figure 1*b*, when the particle is out of trapping focus, the net momentum changes, or net force, can draw the particle back to the centre of the trap. When the particle is located in the centre of the trap, individual rays of light are refracting through the particle symmetrically, resulting in zero net lateral force and cancelling out the scattering force of the laser light (Ashkin & Dziedzic 1987; Svoboda & Block 1994).

If the particle size is substantially less than the wavelength, then the particle is in the Rayleigh regime. The direction of the force is independent of the particle shape and its magnitude varies with the particle orientation. The trapping particle can be considered as an induced dipole and the electromagnetic field of the light pulls the particle towards the brightest part of the beam, where the induced dipole may minimize its energy. In this case, the scattering force is proportional to the optical intensity and points towards the propagation of the laser light, while the gradient force is proportional to the gradient intensity and points in the direction of the intensity gradient. The gradient force attracts the particle into the region of the highest intensity, but the scattering force draws the particle into an equilibrium position that is slightly downstream of the maximum intensity. The competition between the two forces can result in stable trapping (Ashkin 1992).

When the particle sizes are comparable with the wavelength of the trapping laser, neither the ray optic nor the dipole approach is valid. More complete electromagnetic theories are needed for particles in this intermediate size range, although some recent theoretical calculations of forces on a sphere in this regime (0.1–10λ). Because the majority of objects are in this size range (0.1–10λ), such as bacteria, yeast, organelles of larger cells and dielectric microspheres used alone or as handles to manipulate other biological objects, a computational toolbox has been developed for a quantitative description of optical trapping (Nieminen *et al.* 2007).
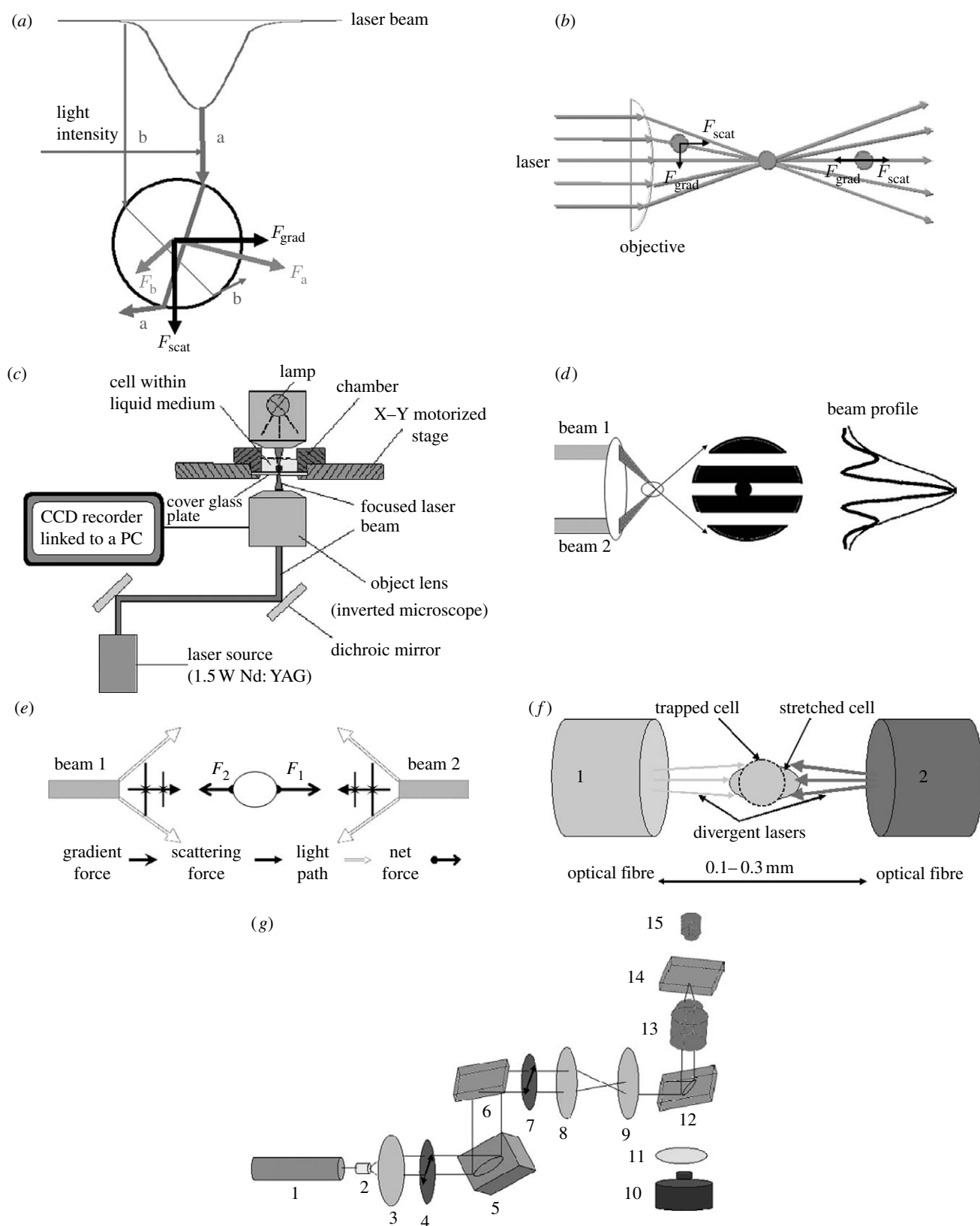
Figure 1. Working principles of optical tweezers. (*a*) The scattering (F_{scat}) and gradient (F_{grad}) components of optical forces on a dielectric sphere due to a Gaussian laser beam (light intensity increases from *b* to *a*). (*b*) Schematic of optical tweezers. Light enters the objective lens of a microscope and is focused to a diffraction-limited beam waist, creating a three-dimensional light gradient; a particle that is out of trap is brought back to the centre of the trap. (*c*) Typical experimental set-up of optical tweezers, adapted from the technical note of Cell Robotic Inc., USA. (*d*) Two-beam interferometric optical tweezers, adapted from Chiou *et al.* (1997). (*e*) Schematic of gradient and scattering forces for two beams, adapted from Constable *et al.* (1993). (*f*) Schematic of optical stretcher, adapted from Guck *et al.* (2000). (*g*) Schematic of holographic optical tweezers generated from a spatial light modulator (SLM), adapted from Martin-Badosa *et al.* (2007). 1, laser beam; 2, LC lens; 3, LE lens; 4, polarizing element; 5, SLM; 6, dichroic mirror; 7, polarizing element; 8, telescope; 9, telescope; 10, CCD camera; 11, tube lens; 12, dichroic mirror; 13, microscopic objective; 14, sample; 15, illumination.

2.2. Trapping force calibration

The trapping forces depend on the intensity of laser power, the shape of laser focus, the size and shape of the trapped particles and the index of refraction of the trapped particles relative to the surrounding medium. It is difficult to measure the trapping forces directly but there are several ways to calibrate them. The forces can be calibrated by a power spectrum of Brownian motion of a trapped particle and the trapping stiffness can be determined (Sheetz 1998; Berg-Sorensen & Flyvbjerg 2004). Another way of calibration is based on the fact that the external forces applied to a single particle within an optical trapping can push a single particle away from the focal region, and the force from the OT usually draws the particle back to the centre of the trap. In the equilibrium position, the external force equals the force from the OT. For a small displacement, the force from the OT, termed as restoring force, can be estimated by

$$F = -kX, \qquad (2.1)$$

where k is the trap stiffness and X is the displacement of the particle away from the centre of the trap, when displacements are smaller than half the radius of the particle within the focal region.

Once the trap stiffness is determined or given, the external force applied on the particle can be determined by accurately monitoring the position of a particle in an optical trap. OT, therefore, have been widely used as a passive force measurement tool. Accurate position detection and measurement are essential for a quantitative optical trapping. Different position detection methods, such as video-based position detection, imaging position detection with a quadrant photodiode (QPD) and laser-based position detection with a QPD, have been reviewed in Neuman & Block (2004). A QPD can measure nanometres displacement at a rate of 10 kHz; therefore, small forces can be measured with a very high time resolution. However, it is difficult to implement a QPD for multiple particles simultaneously. Video cameras allow multi-particle tracking, with an accuracy order of 5 nm and a video acquisition rate of 25–120 Hz. Temporal resolution can be improved through the use of high-speed video cameras (Keen *et al.* 2007) but high-speed video tracking will be ultimately limited because spatial resolution decreases as the frame rate increases (Neuman & Block 2004).

Similar to the method described previously, the drag force method is to apply a known viscous drag force F and measure the displacement X away from the centre. In practice, drag force is usually produced by periodic movement of stage in an either triangular or sine waves of displacement while holding the particle in the trap.

The direct and widely used calibration approach is the escape force method. For a free particle of radius r in solution far away from the surface, knowing the critical velocity v when the particle escapes from the trap, the maximum trapping force F, which equals the opposing viscous drag force according to Svoboda & Block (1994) can be calculated as

$$F = 6\pi\eta rv, \qquad (2.2)$$

where η is the viscosity of the surrounding liquid.

2.3. Instrument

A simple set-up for OT in figure 1*c* is directing a laser beam through the interior of a microscope and filling the back aperture of a microscopic objective. The numerical aperture (NA) equals the index of refraction of the immersion fluid. Typically, the system is implemented using a high NA objective to ensure that true three-dimensional trapping is achieved. The irradiation source is a laser and the most popular power source is Nd:YAG (wavelength of 1064 nm) for single cell applications due to its biological amiability. The detailed discussion for each part of the set-up can be found in a review by Neuman & Block (2004) and a book by Sheetz (1998). Conventional OT use a microscopic objective lens and a standard Gaussian laser beam. Non-Gaussian laser beams, dual beams and multiple traps have been developed for OT so this emerging tool can be widely used in cell manipulation and characterization.

2.3.1. Non-Gaussian laser beams. In conventional OT, the laser intensity profile shows a Gaussian radial distribution; as a result, such a beam can be used to trap a single particle at one time. These conventional techniques have no capacity to tailor the optical potential in a three-dimensional space. A Bessel beam with a radial intensity profile presenting as a zero-order Bessel function has been explored to replace traditional Gaussian beams (Durnin 1987). In contrast to the single (bell-shaped) central maximum of a Gaussian beam, a Bessel beam consists of a bright centre spot surrounded by series of concentric rings of decreasing intensity. By continually reconstructing and supporting this central maximum, the concentric rings of a Bessel beam allow it to maintain its shape and resist spreading, even when an object such as an optically trapped particle lies in its path. Through the use of such a beam as OT, it is possible to trap and manipulate many different particles distributed over a distance of approximately 3 mm simultaneously (Garces-Chavez *et al.* 2002). However, Bessel beams only allow particles to be optically confined within perpendicular two-dimensional planes, and the particles are free to move in the direction of the beam.

A Laguerre–Gaussian mode has been created to obtain a rotating asymmetric intensity profile. This light beam possesses helical wavefronts that carry an orbital angular momentum (Allen *et al.* 1992; He *et al.* 1995). This beam is characterized by an intensity maxima spiral around a dark centre core, that is, a zero on-axis intensity. With their zero on-axis intensity, the axial trapping efficiency of OT has also been improved. The Laguerre–Gaussian beams within OT, termed as 'optical vortices', are able to offer stable three-dimensional confinement of hollow glass spheres from 2 to 50 μm (Gahagan & Swartzlander 1998). Particles that have a lower refractive index than their surrounding media are repelled from the beam axis using a conventional Gaussian beam. This problem can be overcome by the Laguerre–Gaussian beams. The optical vortices can also hold high-index particles to the normal position of just below the beam focus

(Gahagan & Swartzlander 1999). The optical vortex tweezers can also apply controlled torques on trapped objects. The technique is flexible in changing the rotational symmetry of the interference pattern by adjusting the indices of the Laguerre–Gaussian mode, thereby potentially optimizing the shape of the intensity pattern to the shape of the object to be rotated.

2.3.2. Dual beams. Two optical beams, usually produced from a beam splitter, have been widely used to create dual optical traps (Fallman & Axner 1997). This requires that two light paths are controlled by different x–y deflector systems, so it is complicated to control two light beams and hard to achieve position stability. The two beams can be placed either to be parallel or to be counter propagating. Two parallel beams are used to create an interference pattern, as shown in figure 1d, the intensity profile within which gives rise to a gradient force confining both spherical and 'rod-like' particles. This OT is also termed as 'interferometric OT' (Chiou *et al.* 1997). Adjusting the path difference between the two beams results in a translation of the interference pattern and trapping particle. By ensuring the two beams are slightly displaced, the interference patterns can be confined to a centre portion of the field of view with 'non-fringed', high-intensity regions on either side, which could provide complete confinement of manipulated particles. This technique has been applied for trapping simultaneously both low- and high-index particles. MacDonald *et al.* (2003) used a simple-etched hologram to produce a five-beam interference pattern that creates an optical lattice. This three-dimensional optical lattice provides the ability to sort particles through a three-dimensional flow. Ladavac *et al.* (2004) created a complicated sorting sieve based on tailing the relative phases and intensities of the interfering beams. Schonbrun *et al.* (2005) further developed this technique to afford three-dimensional traps by an optical lattice formed by interference of multiple plane waves, which were generated through a single phase-only spatial light modulator (SLM).

Two divergent counter-propagating beams were first used by Ashkin (1970) to demonstrate the first actual trap. Constable *et al.* (1993) tried to place two beams in an exactly counter-propagating way and they provided an equation to calculate the scattering force for these two beams. The gradient and scattering forces are shown in figure 1e. For two identical beams from the opposite side, although the net force ($F_1 - F_2$) or the scattering force exerted on the trapped particle is zero, the surface force stretches the particle with ($F_1 + F_2$)/2 and the stretch force can be up to several hundred pN (Guck *et al.* 2000). This technique is attractive for stretching single cells or single polymer molecules and is known as optical stretching (OS) and can be used to measure the elasticity of biological cells (Guck *et al.* 2000, 2001, 2002), as shown in figure 1f. The advantages include that optical deformation does not require any kind of mechanical contact and covers a stress range previously inaccessible to cell elasticity measurements. Another advantage of using two divergent beams is to reduce photodamage or any

two-photon-induced damage caused by a tightly focused light beam, which will be discussed in §2.4 (Jess *et al.* 2006).

2.3.3. Multiple traps. OT have been configured to create multiple traps so that multiple particles can be trapped simultaneously. These traps can be implemented by splitting the beam early in the optical circuit to produce two separate light paths that are combined before entering the microscope, rapid scanning of a single beam between two or more trapping positions and using computer-generated holograms to produce multiple beams simultaneously.

Two and more beams have been discussed in §2.3.2. Techniques to generate controllable multiple beams have also been developed. The vertical cavity surface-emitting laser (VCSEL) arrays, in which each laser is focused and acts as an individual trap and manipulation source, are able to provide an inexpensive compact package (Flynn *et al.* 2002; Ozkan *et al.* 2003*a,b*). However, they have a relatively low power input. Eriksen *et al.* (2002) used an alternative technique, generalized phase contrast (GPC) and a prefabricated phase mask to generate a laser beam array. A phase-only SLM encodes the desired pattern in the phase component of a collimated and expanded laser beam. This phase-encoded information serves as the input for a GPC system, in which a phase-contrast filter generates a high-contrast intensity pattern that directly corresponds to the phase perturbation of the input wavefront. The intensity pattern is focused using a microscope objective lens for trapping microscopic particles. Another approach used by Rodrigo *et al.* (2003) was based on the Shack–Hartmann wavefront sensor. A beam passes through a phase modulation from a reflection- or transmission-type SLM. Spatial Fourier transformation of the SLM-coded patterns is performed by a lenslet array. Then, the hologram enters the objective lens to be focused to a diffraction-limited spot or a single OT. This straightforward process enables an adjustable number of traps and real-time control of the position, size, shape and intensity of each individual beam in arbitrary arrays by encoding the appropriate phase pattern on the SLM in two and three dimensions (Rodrigo *et al.* 2006).

Scanning techniques generally use acousto-optic deflectors (AODs) that can scan a beam from point to point at kilohertz rates (Visscher *et al.* 1993). The AODs appear to be excellent for two-dimensional optical landscapes. By time sharing the light between trapping sites, the beam must revisit each trapping object often enough that the object has not diffused a significant distance. As a result, a limited number of objects can be manipulated. Up to 20×20 optical traps and partly in three dimensions have been demonstrated by using rapid AODs (Vossen *et al.* 2004).

To achieve true three-dimensional multiple optical traps, one must turn to holographic optical tweezers (HOTs). Multiple optical traps are created by using diffractive optical elements to split and steer the light from a single beam between multiple traps, which can easily become dynamic by using liquid crystal devices,

such as SLMs, to display phase-only holograms (Curtis *et al.* 2002). The working principles of HOTs generated from an SLM are illustrated in figure 1*g* (Martin-Badosa *et al.* 2007). A continuous-wave TEM$_{00}$ laser beam is first expanded and then collimated by two lenses. A pinhole spatially filters the light at the back focal plane of the expander lens to ensure clean Gaussian illumination on the SLM that is designed to modulate the phase of the laser front and it introduces a hologram (a complex diffraction pattern) to the laser light distribution. It may operate by either reflectance or transmittance and is sandwiched between polarizing elements with specific orientations. After passing through a telescope, the beam is reflected upwards by a dichroic mirror and is focused by the high NA microscope objective on the sample plane. HOTs offer complete flexibility in manipulating multiple particles independently through the creation of arbitrary optical landscapes and other modes of light such as optical vortices can be created (Curtis & Grier 2003). Advanced SLM technology and real-time hologram calculation algorithms have allowed the creation of an array of up to 400 optical traps (Curtis *et al.* 2002).

Multiple traps have been able to be created by the three methods described above; however, their characterization and calibration simultaneously remains challenging. Theoretical approaches have been developed for absolute and precise calibration for a single beam (Hansen *et al.* 2006; Viana *et al.* 2007) and those models will be extended for multiple traps. Experimental methods using a QDP to detect the nanometre resolution displacement of beads have been used to characterize and calibrate multiple traps (Guilford *et al.* 2004; Dharmadhikari *et al.* 2007). However, it is challenging to track many particles simultaneously using a QDP. A high-speed video camera was used for multiple traps and centre-of-mass tracking was adopted to avoid out-of-memory problems (Keen *et al.* 2007). This high-speed camera could be very useful to characterize and calibrate multiple traps.

2.3.4. OT in combination with other instruments. Other enabling techniques have been combined with OT to allow exploring further applications of OT. Sensitive position detection is an essential tool for quantitative optical trapping as nanoscale measurement of both force and displacement relies on a well-calibrated system for determining position. This position detection technique allows calibration of the trap to work out the trapping stiffness from equation (2.1). This is especially useful for multiple traps, like for scanning multiple traps or HOTs, as the drag force calibration method discussed in §2.2 is not feasible for multiple traps. After the trapping stiffness is given, the position displacement of a particle in an optical trap can be used to work out the forces applied on the particle. Therefore, position detection is an essential part for OT as a force measurement tool. A review of position detection techniques has been introduced by Neuman & Block (2004). The position-sensing capacities for optical traps have been pushed to angstrom precision, and

one is able to observe a distance of approximately 3.4 Å (Abbondanzieri *et al.* 2005; Greenleaf *et al.* 2005). Rohrbach (2005) has measured a controlled 25 fN force on a 533 nm latex sphere. This suggests that OT can be applied to measure the smallest forces that cannot be achieved by traditional AFM and other tools.

Raman spectroscopy can provide information about chemical bonds in molecules by identifying spectral patterns excited by a near-infrared laser beam. Therefore, OT are often combined with Raman spectroscopy to provide essential intracellular information (Xie *et al.* 2002, 2005; Creely *et al.* 2005; Jess *et al.* 2006). Other techniques, such as total internal reflection microscopy (TIFT; Oheim & Schapper 2005), confocal microscopy (Hoffmann *et al.* 2000) and cellular microscopy (Emiliani *et al.* 2005), have been reported to combine with OT.

Microfluidics is another area where OT show great promise for its application. Microfluidic channels offer a fluid flow system with sample volume as small as the order of a few nanolitres where cells can be transported, manipulated, sorted and isolated with their surrounding media. OT as an important contact-free cell-friendly manipulation tool have been integrated with microfluidic devices (Enger *et al.* 2004; Paterson *et al.* 2005; Wang *et al.* 2005; Jess *et al.* 2006; Monat *et al.* 2008).

2.4. Intricate problems: heating and photodamage

Laser adsorption by the sample can lead to damage or 'opticution' as a highly focused spot with power intensities of megawatts per square centimetre is used for OT (Dholakia & Reece 2006). This may occur with both one- and two-photon processes. Wavelength is an important issue when biological cells are trapped. The photodamage throughout the near infrared region favoured for optical trapping (790–1064 nm) was investigated and the action spectrum for photodamage exhibited minima at 830 and 970 nm and maxima at 870 and 930 nm for both *E. coli* (Neuman *et al.* 1999) and Chinese hamster ovary cells (Liang *et al.* 1996). However, the damage was reduced to background levels under anaerobic conditions, implicating oxygen in the photodamage pathway (Neuman *et al.* 1999). Even at a wavelength of 1064 nm, the division and growth of *E. coli* cells were affected when cells were radiated to OT by using an on-chip cultivation system (Ayano *et al.* 2006).

Shorter wavelengths below 800 nm can also bring great damage to biological cells that were observed by Konig *et al.* (1996*a*,*b*) and Leitz *et al.* (2002). Leitz *et al.* (2002) systematically investigated effects of illumination from OT by using different laser powers, irradiation time and wavelength on cell damage. A transgenic strain of *Caenorhabditis elegans*, which had been used as a sensitive biomonitor responsive to various types of external stresses, carried a reporter gene (*E. coli* lacZ) that was under the transcriptional control of a specific heat shock promoter. By exposing the cells to illumination from the OT at wavelengths from 700 to 850 nm for 30–240 s, the highest frequency of induction of

the gene expression activated by the gene promoter was found to be at 760 nm laser radiation mainly due to photochemical effects. At a wavelength above 800 nm, the cell damage was found to be mainly due to photothermal effects.

The thermal effects on cells from high photon intensities can be seen by direct temperature rise. When using 100 mW laser tweezers (1064 nm in wavelength), the trap-induced temperature increase is between 1 and 2°C. In trapped human sperm cells, hamster ovary cells and liposomes, the temperature increases were measured to be of the order of 10, 11.5 and 14.5°C W^{-1}, respectively (Liu *et al.* 1995, 1996). This is confirmed by Peterman *et al.* (2003). This effect has also been investigated by cell metabolic activities. Tethering a single *E. coli* cell to a glass cover-slip by a single flagellum so that the single cell rotates at a rate proportional to its membrane proton potential, then monitoring the rotational rates of the single cell subjected to laser illumination is a rapid and quantitative measure of its metabolic states.

To reduce photodamaging effects of OT to cells, near-infrared lasers such as Nd:YAG (1064 nm in wavelength), Nd:YLF and diode or Ti:sapphire lasers can be chosen as the laser source. Alternatively, the laser can strike on particles rather than cells to avoid direct contact between photons and cells by attaching one or more particles to cells. Apart from these methods, two divergent optical beams rather than a single highly focused beam are used for reducing the photodamage in optical trapping. To reduce the heating effect, heavy water (D$_2$O) rather than usual water can be used because it absorbs less than usual water over typical trapping wavelengths. At a wavelength of 780 nm, the absorption coefficients for D$_2$O are two orders of magnitude smaller than those for H$_2$O (Dholakia & Reece 2006).

3. APPLICATIONS FOR SINGLE CELLS

3.1. *Active nanomanipulation*

OT have been widely employed as a tool for actively manipulating and positioning biological objects at the nano/microscale. One of the most popular applications is to apply tweezers to confine or constrain single cells, as well as to organize, assemble, locate, sort and modify them.

3.1.1. Positioning cells. OT have been used to hold cells in a static or fluid flow environment. The simple application was to measure volume changes of a single isolated kidney cell under osmotic shock and a phenomenological analysis of water transport. A single Madin-Darby canine kidney cell was grabbed and suspended in liquid without touching either the glass substrate or other cells with the aid of OT (Lucio *et al.* 2003). Water permeability, osmotic influx rate and regulatory volume were obtained by using videomicroscopy with digital image analysis.

When a single cell is trapped by OT, light hitting the cell surface changes the intensity and direction of the bouncing photons. The intensity of scattered light from A375 cells, lymphocytes and granulocytes was recorded over an angular range of 0.5–179.5° with 30 ms time resolution and exhibited a significant and complex time dependence (Watson *et al.* 2004). The specific diagram of light scattering for a single cell within an optical trap can be used to identify different internal structures of the cell, distinguish living cells from dead cells and separate cells based on the differences of cell size, shape, refractive index and morphology.

By capturing a single cell in an optical trap, Raman spectrometry has been used to provide essential intracellular information for a single cell. This technique has been used for single biological cells (Xie *et al.* 2002) and this group further applied this technique to identify and discriminate six different bacterial species at various growth conditions (Xie *et al.* 2005). The highly reproducible biomolecular fingerprint of each cell provided from the instrument has been successfully applied to distinguish normal human lymphocytes from transformed Jurkat and Raji lymphocyte cell lines (Chan *et al.* 2006) and cancer cells from normal cells (Zheng *et al.* 2007). This technique could be applied to study identification, differentiation and maturation of stem cells.

Singh *et al.* (2005) used this technique for a quantitative study of the fermentation process for a single yeast cell in real time, so that real-time monitoring of cell biochemistry can be achieved. However, the cell will generally rotate in a trap about the trapping axis (Grover *et al.* 2000); multiple beams around the periphery of the cell have been used to provide a stable trap. Creely *et al.* (2005) used HOTs to stably trap Jurkat cells in suspension, and scan back and forth across the focus of the stationary excitation beam. In this way, the space-resolved spectra of entire cells have been obtained. Jess *et al.* (2006) adopted a similar technique, but chose two divergent beams to confine a primary human keratinocyte cell and recorded separate spectra from the membrane, cytoplasm and the nucleus.

By combining micro-Raman spectroscopy with OT and a microfluidic system, the oxygenation cycle of a single RBC can be selectively trapped by OT and monitored in real time while different buffers were transported through a microfluidic channel using electro-osmotic flow (Ramser *et al.* 2005). This technique holds potential for *in vitro* monitoring of cellular drug response by feeding the pharmaceutical solution to the fixed cells and measuring physical and chemical changes in cellular components.

3.1.2. Cell transportation. OT are able to move single cells in a liquid medium without contact. This unique feature is highly desirable for cell manipulation in sterile conditions. OT have been applied to relocate neuron cells to form cell groups (Townes-Anderson *et al.* 1998). Some of the neuron cells were cultured on the adherent side of a culture dish and others on the less adhesive side. Unattached cells were trapped and relocated next to cells lying on an adhesive culture substrate to allow interactions among cells. For example, when a rod cell was relocated to a group

containing a cone cell and a multipolar neuron, then it was found that prominent growth of the neuron was inhibited by the relocated rod cell. Optical trapping did not affect the ability of neurons to subsequently attach to the culture substrate, and organelles, nuclear and cytoplasmic structure of manipulated cells were completely normal. OT provide a benign tool for micromanipulating whole neurons.

Arrayed cells can also be moved by VCSEL arrays that were used as a miniaturized source of infrared light for remote manipulation (Ozkan *et al.* 2003*a,b*). 3T3 mouse fibroblasts and primary rat hepatocytes were transported into a specific location. This system allows capturing selected individual or multiple cells and performing conventional molecular characterization. The limitation is that only cells smaller than 10 μm in size can be moved using the current VCSEL-driven OT. Since large arrays (32×32) of VCSELs are now commercially available, this system has the potential to be extended to the parallel manipulation of many cells simultaneously.

Wakamoto *et al.* (2001) reported the building of two microchambers for analysis and cultivation, the two chambers being connected through a narrow channel through which a single *E. coli* cell was trapped and transported by OT. After an *E. coli* cell in the analysis chamber was divided into two daughter cells, one daughter cell was trapped and transported into the cultivation chamber for further differentiation. This technique allows comparing genetically identical cells under contamination-free environment, which will shed light on heterogeneous phenomena such as unequal cell division. Enger *et al.* (2004) designed a similar system so that *E. coli* cells were moved between reservoirs filled with different media on a time scale of a few seconds. It was found that there was no contamination when cells were dragged to a place with a different liquid medium and then transferred back again from different channels. This group (Eriksson *et al.* 2007) used this technique to investigate the cell response to a sharp glucose concentration gradient between the two channels in which 25 yeast cells were moved back and forth between the two media by holographic OT. This provides a new method to investigate real-time cell responses to various extracellular environment conditions without being removed from the field of view of the microscope.

3.1.3. Cell sorting.

A traditional and widely used method to sort and fraction cells is fluorescence-activated cell sorting (FACS; Herzenberg *et al.* 2002). The cells are to be chosen from the decision based on the fluorescence signal from the detection region. This is termed as 'active sorting' (Dholakia *et al.* 2007) as some markers have to be attached to the cells. While hydrodynamic focusing is maintained for a macroscopic FACS machine, optical force is used for cell deflection of microfluidic FACS (figure 2). Buican *et al.* (1987) pioneered the use of a deflection beam to separate cells and a propulsion beam to maintain the travelling path of separated cells up to several millimetres. Ozkan *et al.* (2003*b*) designed a T-type microchannel junction for
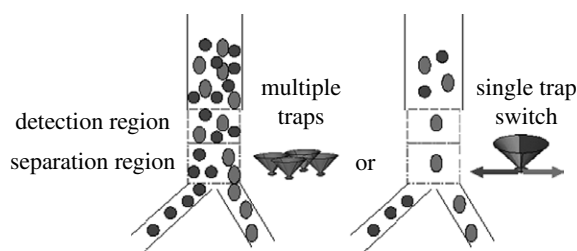

Figure 2. Optical tweezers for cell sorting. Targeted cells are detected in the detection region and identification of those cells triggers switching on either multiple traps or single trap. Cells are driven by optical tweezers to be delivered to the collection output while all other cells flow to the waste output. Adapted from Wang *et al.* (2005).

transporting cell solution and used VCSEL-driven OT to trap and deliver several target cells to a collection reservoir simultaneously. Similarly, Enger *et al.* (2004) used a Y-type junction coupled with OT for cell separation. In these reports, only a few cells were used and laser beams were manually operated to demonstrate the concept.

A functional microfluidic FACS has been reported by Wang *et al.* (2005). Two laser sources have been used in this cell sorter: a near-infrared laser for the optical switch and a visible wavelength laser for the detection and fluorescence measurement. Cells flowing in from the sample input were aligned to a narrow stream by hydrodynamic focusing. First, cells in the focused flow passed into the analytical region and then through the optical switch region. When a cell was detected and determined to be a target cell, an acousto-optical modulator was triggered to switch the cell based on a gating of fluorescence signal. A focused laser spot deflected the cell to the target output channel. The cells without being subjected to a laser beam flew out to the waste channel. For example, the cells from a stable-transfected HeLa cell line constitutively expressing a fused histone-green fluorescent protein and non-expressing parental HeLa cells were mixed and separated by passing through the cell sorter. High purity in the collection channel was obtained in varied starting ratios of target cells and the recovery rate was above 85% except in the case of high throughput of 10^6 cells s^{-1}.

Other active sorting techniques, such as simple cell identification by video microscopy and cell deflection by multiple-beam OT, have been developed (Ericsson *et al.* 2000; Grover *et al.* 2001; Oakey *et al.* 2002; Rodrigo *et al.* 2003; Applegate *et al.* 2006). For example, Grover *et al.* (2001) used an image-processing technique for single cell identification and a counter-propagating dual beam to separate blood cells; Applegate *et al.* (2004) generated a line trap, rather than a point trap, by focusing a diode bar, and bovine RBCs were captured by the line trap and directed with an angle to chosen flow streamlines through a seven-channel sorting device; they further wrote about an integrated optical waveguide within two channels for exciting fluorescent-dyed particles and generating microfluidic FACS (Applegate *et al.* 2006). Cran-McGreehin *et al.* (2006) integrated microfluidic channels with semiconductor laser materials, which allow detecting particles and

distinguishing between different sizes by measuring the power or photocurrent reduction due to the presence of a particle in the beam path.

Passive sorting is a marker-free approach, which has advantages of keeping cells in their untouched state (Dholakia *et al.* 2007). There is no need to develop an appropriate marker for cells and to remove markers after separation. Without specific markers, selectivity is based on size, shape and refractive index difference. Within a microfluidic channel, cells are sorted via a size- and shape-dependent gradient force in competition with a size- and shape-dependent viscous drag force. MacDonald *et al.* (2003, 2004) demonstrated the separation of erythrocytes from lymphocytes based on shape difference by using an angled optical lattice that can be extended to any general two- or three-dimensional potential energy landscapes (Ladavac *et al.* 2004; Milne *et al.* 2007; Smith *et al.* 2007).

Cells can also be separated due to the interplay between the radiation pressure and fluid drag, termed as 'optical chromatography' as proposed by Imasaka *et al.* (1995). In this case, a weakly focused laser beam is installed in the counter-propagating fluid flow. When cells flow along the channel, the scattering force from the laser beam pushes cells into the focal region of the laser beam. The net force between the scattering and drag forces results in different equilibrium positions for different cells. This method can be used to separate a range of cells including blood cells (Kaneta *et al.* 1997), bacterial spores and cells (Hart *et al.* 2006, 2007) and pollen (Terray *et al.* 2005).

Passive optical sorting can also be achieved without fluid flow. The Bessel beam has been used for flow-free optical separation of lymphocytes from erythrocytes (Paterson *et al.* 2005) using its unique optical landscape, which has been discussed in §2.3.1. When higher power was used, the biconcave-shaped erythrocytes locked into outer rings of the Bessel beam (third, fourth and fifth), while spherically shaped lymphocytes rapidly moved directly to the beam centre and they were collected from the centre core. Zemanek *et al.* (2004) described using a three-beam interference light field to locate big particles in intensity minimum but small particles in intensity maximum. A size-selective optical-moving pattern is a more productive way to enhance separation, such as a vibrating fringe pattern (Ricardez-Vargas *et al.* 2006), a moving periodic light pattern (Cizmar *et al.* 2006) and time-dependent optical potential energy landscape (Libal *et al.* 2006; Smith *et al.* 2007).

3.1.4. Assembling and organizing cells. OT can be used to relocate, assemble and organize cells so that a group of cells can be formed into a new structure. An optical trap can be used to grab an object which in turn could be used to grab other objects. A microsphere of 5 µm in diameter was trapped first and then used as a handle to trap and manipulate several microspheres (approx. 2 µm in diameter). The assembly of microspheres remained stable as it moved inside a 100 µm channel (Ozkan *et al.* 2003b). This technique can be used to

select and place multiple objectives for optically assisting self-assembly processes.

The assembly function of OT can also be realized through computer-controlled SLMs built on holographic OT because this technique allows manipulating particles both laterally and axially over several tens of micrometres so that particles can be rearranged into three-dimensional configurations. This assembly function has been demonstrated with 18 trapped silica spheres positioned to form a diamond lattice with a unit cell size of 15 µm and four glass beads trapped in the corners of an imaginary tetrahedron by Leach *et al.* (2004). This group has applied the technique to move individual *E. coli* cells in liquid gelatin at predefined positions. When the cells were fixed in place, the lasers were switched off. The three-dimensional configurations of cells within a gelatin sample at predefined positions remained intact for many days. The cells survived within the gelatin matrix for several days when appropriate nutrients were provided. This technique can be used to help in understanding the role of position, proximity and the number of neighbouring cells, not only in cell culture but also in cell differentiation. The ability to form such viable three-dimensional structures will open a wide range of future applications, including the arrangement of various cell types in complex architectures, as motifs for promoting tissue differentiation and growth within the field of cell engineering (Jordan *et al.* 2005).

Using arrays of time-multiplexed holographic OT with a combination of SLM and AOD, Akselrod *et al.* (2006) demonstrated the assembly of three-dimensional heterotypic microarrays consisting of a Swiss 3T3 mouse fibroblast surrounded by a ring of *Pseudomonas aeruginosa* bacteria. The mammalian cell was trapped with nine 2 mW beams, and 16 single 2 mW beams were dedicated to 16 bacteria and all cells were detected to remain viable. The cell-to-cell distance was able to be controlled to less than 400 nm. This technique allows investigating the bacterial infection process through control of colonization and the biochemical library in the microenvironment of a cell and it also has a huge impact on tissue engineering and synthetic biology.

3.1.5. Laser scissors/scalpels and opto-injection. OT can be combined with UV or Nd:YAG laser microbeams to function as scalpels or scissors, which allows precise cutting with submicrometre resolution (Colombelli *et al.* 2004). Novel surgery tools coupled with OT perform separation of individual cells from cell clusters (Leitz *et al.* 2003) as well as dissection of cellular organelles, cytoskeletal filaments (Kumar *et al.* 2006) or chromosomes (Berns *et al.* 1989; Berns 1998).

Transient permeabilization of cell membranes by short-time laser irradiation allows cell fusion and molecular injection (opto-injection). Steubing *et al.* (1991) pioneered bringing two cells into contact in an optical trap and then fusing them by cutting the common wall of the two cells with several pulses of UV laser microbeams. This method provides an effective way of generating hybrid cells without losing cell functions and has been used to selectively transport

individual sperm to its eventual contact with oocytes (Schopper *et al.* 1999).

Opto-injection involves the locally restricted short-term opening of a cell membrane by focusing a single ultraviolet pulse on the phospholipid bilayer so that foreign species in the external solution can be injected or flowed into the cell in a passive manner. Florescent biomolecules have been injected into the cytosol and nucleus of Neuro-2A mouse neuroblastoma cells (Stuhrmann *et al.* 2006).

3.1.6. Optical guiding. OT have also been used for neuronal cell growth, where laser radiation focused on the leading edge of an actively advancing growth cone affects intracellular processes and induces growth towards the laser focus at wavelengths in the range of 800–900 nm. PC12 cells, a neuron precursor cell line, were reported to respond to light by growth towards a laser beam at a wavelength of 800 nm and a relatively low power (Ehrlicher *et al.* 2002). This optical-guiding process occurs as the light pools actin monomers and provides nucleation sites for actin polymerization, which is the driving force for neuronal growth (Ehrlicher *et al.* 2002; Dent & Gertler 2003). Other cell types reported for this optical-guiding process include N1E-115 cells from a neuroblastoma tumour (Mohanty *et al.* 2005*b*), NG108, a rat/mouse hybrid neuroblastoma cell line that produces active growth cones (Stevenson *et al.* 2006), as well as primary embryonic chicken retina cells (Stuhrmann *et al.* 2006).

3.2. Passive piconewton force measurement for single cells

Owing to their precisely controllable force-exerting characteristics, OT are often used for a variety of mechanical force measurements in the pN range for single cells. Although most cells are not conducive to direct optical tweezing due to their size, shape and adherent properties, a small number of cell types such as yeast cells, RBCs and spermatozoa are readily tweezed and provide model systems for force studies (Dholakia & Reece 2006). For those cells that cannot easily be tweezed, the use of microspheres as handles for force probes has allowed the measurement of cellular properties such as membrane tension.

3.2.1. Deformability measurement of unilamellar vesicles. Unilamellar vesicles, composed of a phospholipid bilayer that is the main constituent of biological membranes, have been widely accepted as a model for cell mechanical studies (Ichikawa & Yoshikawa 2001). The mechanical deformation of vesicles by OT was characterized (Foo *et al.* 2004) and the thermal effect on the deformation was investigated (Foo *et al.* 2003). This provides essential information on coupled thermal and hydrodynamics effects on the biomechanical properties of biological cell membrane in physiological flow. OT can also excite lipid bilayers and result in the dynamic instabilities and shape transformations of liposomes under laser trapping (Bar-Ziv *et al.* 1998).

3.2.2. Mechanical characterization of RBCs. The changes in the elastic and viscoelastic properties in RBCs are often correlated with the manner in which the cells respond to structural and molecular alterations induced by the onset and progression of a disease (Suresh *et al.* 2005). The elastic and viscoelastic properties of healthy and infected RBCs have been investigated using OT. By fixing one side of an RBC membrane and pulling the other side with aid of OT, the cell membrane is deformed. The cell deformation under certain force can be used to calculate the mechanical properties (shear modulus), as shown in figure 3. OT have also been used to calculate the relaxation time for RBCs, which is the duration from a distorted shape back to its original one. Using three optical traps to deform RBCs into a parachute shape and then removing all three optical traps, the shape recovery was recorded and the relaxation time was obtained for the cell. The experimental measurement of shear modulus and relaxation time from different groups are summarized in table 2. It can be seen from table 2 that by comparing the shear modulus of different cells, a single healthy RBC can be distinguished from a malaria-infected RBC. The shear modulus of infected RBCs at a late stage was found to be up to an order of magnitude higher than that of healthy RBCs.

Apart from stretching bead-attached RBCs, the cells can also be stretched by two counter-propagating divergent beams, which has been carried out by Guck *et al.* (2000, 2001, 2002). The stretching force can be up to several hundreds of piconewtons and a deformation of up to 80% was observed by this method. They further applied this method to detect changes in the deformability of cells as a function of cancer progression (Guck *et al.* 2005).

Rotation and folding of RBCs have also been investigated by optical traps. Mohanty *et al.* (2004, 2005*a*) observed that in hypertonic buffer, a normal round RBC rotated when trapped by OT and the rotational speed increases linearly at lower trap beam powers and more rapidly at higher powers. By contrast, a malarial parasite-infected RBC did not rotate under the same experimental conditions. The rotational speeds of other RBCs from malaria-infected samples were found to be an order of magnitude less than that of normal RBCs and also increased much more slowly with an increase in trap beam power than that of normal RBCs. When a single live RBC is placed in an optical trap, the normal and infected bioconcave shape of RBCs has been observed to fold into a rod-like shape. If the laser beam is circularly polarized, the folded normal and infected RBCs rotate. However, normal RBCs did not respond to a linearly polarized light while infected RBCs were able to rotate. Rotation speed of the infected RBCs varied from $19g$ to $300g$ and appeared to depend on the stage of infection. Fast rotation was observed at the early trophozoite stage whereas slow rotation occurred at the mature schizonts stage (Dharmadhikari *et al.* 2004).

Recently, Gu *et al.* (2007) developed a single beam near-field laser trapping technique using focused evanescent wave illumination to stretch, rotate and fold RBCs. The ratio of deformation from its original

Table 2. Experimental studies of human red blood cells (RBCs) by optical tweezers.

authors	experimental methods	major findings
Bronkhorst *et al.* (1995)	RBC was vertically oriented in three traps and then the middle trap moved at very low speed to change the cell shape. Finally, all traps were removed and the cell relaxed to its original shape	'young' cells have shorter (162 ms) and 'old' cells have longer (353 ms) relaxation times compared with the total population (271 ms). The relaxation time is markedly shorter (114 ms) when the plasma surrounding the cells is replaced by a phosphate-buffered saline solution
Henon *et al.* (1999)	force generated between 10 and 15 pN	shear modulus of $2.5 \pm 0.4\ \mu\mathrm{N\ m^{-1}}$ for both discotic and nearly spherical swollen cells
Sleep *et al.* (1999)	two independently movable single-beam traps on two beads attached to cells and bead positions detected by a photodiode quadrant detector	shear modulus of $200\ \mu\mathrm{N\ m^{-1}}$ for unmodified cell ghost and $200\ \mu\mathrm{N\ m^{-1}}$ for modified cells by chymotrypsin, PCMS and NEM. For chymotrypsin-treated cells, by imposing a series of stretches, cells relaxed to a condition of a near equilibrium tension after each stretch
Guck *et al.* (2000, 2001, 2002)	two counter-propagating divergent beams providing a stretching force up to 400 pN	shear modulus of $13.0 \pm 5.0\ \mu\mathrm{N\ m^{-1}}$ for spherical cells and a relative increase of radius up to 14% below a stress of $1.47\ \mathrm{N\ m^{-2}}$; nonlinear distortion above a stress of $2\ \mathrm{N\ m^{-2}}$, a relative increase in radius up to 82% at a stress of $2.55\ \mathrm{N\ m^{-2}}$
Lenormand *et al.* (2001)	three optical traps were used for a blood cell via three beads bound to its membrane	area expansion modulus of $4.8 \pm 2.7\ \mu\mathrm{N\ m^{-1}}$, and shear modulus of $2.4 \pm 0.7\ \mu\mathrm{N\ m^{-1}}$ for the spectrin skeleton in low hypotonic buffer ($25\ \mathrm{mOsm\ kg^{-1}}$), and both values were higher in isotonic buffer
Dao *et al.* (2003) and Lim *et al.* (2004*a,b*)	laser light was directed on larger beads ($4.12\ \mu\mathrm{m}$) attached to the cell membrane and the procedure was as described in figure 3*a–c*. The maximum force was estimated to be approximately 193 ± 20 pN	the shear modulus at larger strain was estimated to be $5.5\ \mu\mathrm{N\ m^{-1}}$ when the force was exerted up to 85 pN. The largest deformation of 50% was achieved
Suresh *et al.* (2005)	RBCs infected by *Plasmodium falciparum* at different erythrocytic developmental stages (ring, trophozoite and schizont stages) were subjected to optical forces up to 150 pN	elastic shear modulus for infected RBC at ring, trophozoite and schizont stages of 16, 21.3 and $53.3\ \mu\mathrm{N\ m^{-1}}$, respectively
Li *et al.* (2006)	force ranging from 0 to 16 pN	shear modulus of $4.6\text{–}5.2\ \mu\mathrm{N\ m^{-1}}$
Gu *et al.* (2007)	a single beam near-field optical trap to rotate, stretch and fold RBCs	rotational speed increased up to $1.6g$ and folding angle increased up to 60° as the power increased; ratio of deformation by stretching up to 23%

size was as large as approximately 23%. Both rotation and folding of the RBCs were linearly increased as the laser power increased.

One should note that most of the experimental results in table 2 were obtained at room temperature and those results may not truly reflect the deformation of RBCs in the human body. It has been found that the mechanical properties of RBCs can be changed due to temperature change in the human body (Waugh & Evans 1979). Foo *et al.* (2006) investigated the effect of heating and cooling on mechanical properties of a single RBC trapped by OT. It was found that the extra deformation under hydrodynamic flow for an RBC at body temperature (37°C) was significantly higher than that at room temperature. When heating the liquid medium from 23 to 42°C and then cooling back to 23°C, the degree of RBC deformation was found to be irreversible and the RBC became much softer, which may be due to the irreversible transformation of the membrane molecular structures.

3.2.3. Mammalian cells with intracellular organelles. Unlike simple bilayers in model lipid vesicles and RBCs, other human cells are coupled with the cell cytoskeleton and extracellular environment via molecular interactions including lipid–protein bonds, transmembrane protein linkage to cytoskeleton and the extracellular matrix. Similar to human RBCs, OT have also been applied to study the mechanical properties of cell membranes. Tether extraction is the most accurate method to quantitatively characterize the plasma membrane. To form a membrane tether, micrometre-sized beads are typically used as handles to grab the cell membrane. The force to manipulate the bead can be quantitatively obtained from OT.

The tether formation force of a single OT-stretched chondrocyte cell was measured to be approximately 232 pN when cells were cultured after 1 hour while it was 591 pN after 6 hour. The culture time was found to have a significant effect on the chondrocyte cell adhesion process (Huang *et al.* 2003). A bigger tether
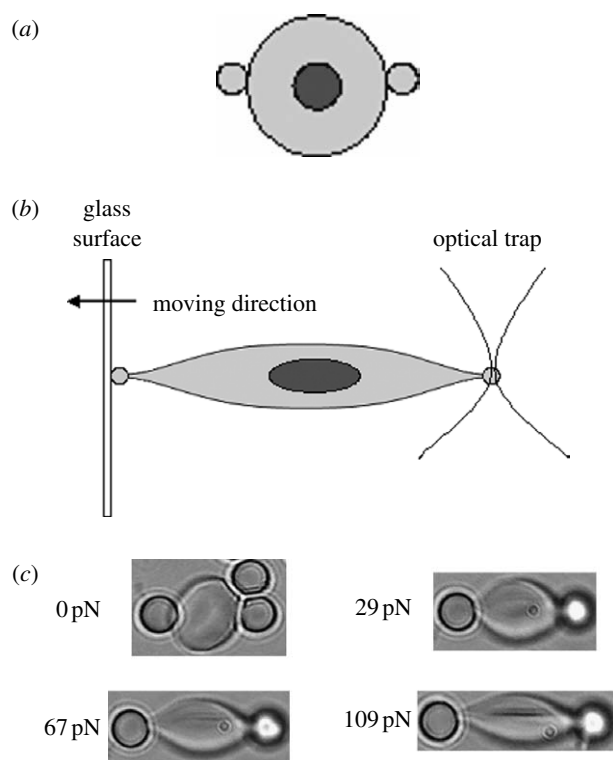
(a)

(b) glass surface

optical trap

moving direction

(c)

0 pN

29 pN

67 pN

109 pN

Figure 3. Stretching RBCs by optical tweezers. (a) Two diametrically opposed silica beads of 4.1 µm are attached onto an RBC surface. (b) One bead is trapped by optical tweezers while the other is fixed onto a glass surface. Deformation is achieved by moving the glass surface to the opposite direction. (c) Large deformations of RBCs in phosphate buffer saline solution at room temperature are captured by optical micrographs under different trapping forces. Adapted from Lim *et al.* (2004*a*).

formation force for outer hair cells from the lateral wall (499 ± 152 pN) than that from the basal end (142 ± 49 pN) was consistent with an extensive cytoskeletal framework associated with the lateral wall (Li *et al.* 2002).

The membrane mechanics of human mesenchymal stem cells (hMSCs) has been shown to critically affect MSC differentiation. The average tether lengths were found as 10.6 ± 1.1 µm for hMSCs and 3.0 ± 0.5 µm for fibroblasts measured by using OT stretching. During tether elongation, the extraction force on the bead fluctuated around a constant value and this demonstrated that there was a small bilayer reservoir on the membrane to buffer minor fluctuations in the membrane tension (Titushkin & Cho 2006).

Membrane mechanics directly affects cell adhesion and reorientation. Curtis & Spatz (2004) applied holographic OT techniques to study hyaluronan-mediated adhesion processes of chondrocyte cells. The early stage cells had reversible adhesion with negatively charged and fibronectin-coated microspheres even after they were held at the cell surface for 10 s. By contrast, late-stage cells stuck irreversibly to all types of beads: positive, negative, fibronectin and hyaluronan coated. Additionally, only the late-stage cells produced membrane tethers. These observations suggest that the late-stage chondrocytes have less surface associated with hyaluronan and have interesting implications for the role of hyaluronan in the early stages of cell

adhesion. Other reports on using OT for cell adhesion include short-term binding of fibroblasts to fibronectin-coated glass (Thoumine *et al.* 2000), haematopoietic stem cells adherent to the host bone marrow micro-environment (Askenasy & Farkas 2002), macrophages adherent to different polymer templates for growing artificial artery grafts (Knoner *et al.* 2006) and human bone cells attached to implant surfaces (Andersson *et al.* 2007*a*).

OT can also offer a well-defined piconewton force on a single cell, which allows investigating cell response to defined load or stress. Walker *et al.* (1999) used a single optical trap to exert 7 pN force on bone- and cartilage-derived cells. Changes in intracellular calcium levels were observed using Fluo-3 labelling. Human-derived osteoblasts responded to optical trap force with an immediate increase in calcium concentration. Response to the same force by the different bone- and cartilage-derived cells varied from 2% (chondrocyte) to 50% (human osteoblast) increase in fluorescent intensity.

OT have also been used for manipulating and determining the force generation and swimming properties of sperm. Nascimento *et al.* (2006) described the effects of laser trap duration and laser trapping power on sperm motility between sperm swimming force, swimming speed and speed of progression score and concluded that sperm swimming forces measured by optical trapping provide new and valuable quantitative information to assess sperm motility. Shi *et al.* (2006) developed a real-time tracking system for single sperm under optical traps and Shao *et al.* (2007) used a three-dimensional ring-shaped optical trap to characterize sperm mobility.

3.2.4. Mechanical properties of microbiological cells. Microbiological cells have been widely used for optical manipulation (Ashkin & Dziedzic 1987; Leach *et al.* 2004; Singh *et al.* 2005; Hart *et al.* 2006, 2007). OT have also been a quantitative tool for the measurement of mechanical properties of micro-organisms as they can trap objects as small as 5 nm and exert forces exceeding 100 pN (Grier 2003). The optical method allows investigating the mechanical properties of some components of bacterial cells, such as tether formation, mechanical behaviour of individual P pili, twitching mobility of pilus and flagella rotation.

Tethers can be formed between a living *E. coli* cell and a bead by unspecifically attaching the bead to the outer membrane and pulling it away using OT. These tethers were measured to be tens of micrometres long, several times the bacterial length. Visco-elastic tether force–extension relationships were observed: a spring constant of $10\text{–}12$ pN μm^{-1} was reported for the first pulling of tethers while it decreased to $6\text{–}7$ pN μm^{-1} for subsequent pulling of tethers and typical relaxation time scales of hundreds of seconds were reported. This unspecific tethered attachment mechanism could be important in the initiation of bacterial adhesion (Jauffred *et al.* 2007).

The adhesion of micro-organisms to the surface of host tissue is often a precursor in pathogenesis. In this process, bacterial pili are responsible for mediating

adhesion and maintaining bacteria–host contact during the early stage of an infection. Jass *et al.* (2004) investigated the mechanical behaviour of individual P pili of a uropathogenic *E. coli*. Three elongation regions of P pili were identified. In region I, P pili stretched elastically up to an averaged relative elongation of 16%. In region II, the pili unfolded their helix structure and the elongation was found to be under constant force. This unfolding elongated the pilus up to approximately seven times its unstretched length. In region III, pili elongated in a nonlinear manner as a result of stretching until the bond ruptured. These findings suggest that bacterial pili can withstand tension over a broad range of lengths. Andersson *et al.* (2007*b*) compared P pili and type I pili of uropathogenic *E. coli* in the urinary tract by in-site measurement: a similar unfolding force of 30 pN was found and an elongational speed of 6 nm s^{-1} for type I pili and 400 nm s^{-1} for P pili. The quantitative data can be used to understand the infection process and design novel drugs for bacterial infection.

Type IV pilus is also involved in bacterial cell adhesion to host mammalian cells as well as bacterial motility. OT have been used to measure the pilus retraction and elongation at a resolution of several nanometres. A single pilus from bacterial cells can generate a force in excess of 100 pN making pili the strongest linear motors (Maier *et al.* 2004; Maier 2005).

Interaction between bacterial cell and surface can also be characterized. Liang *et al.* (2000) quantified the adhesion forces from the interaction of uropathogenic *E. coli* to self-assembled monolayers (SAMs) by breaking a single interaction of approximately 1.7 pN between pilus and mannose groups linked to the SAM. Fallman *et al.* (2004) measured the binding forces of *E. coli* cells to galabiose-functionalized beads. Forces of 10–15 pN, when the starting position of the bacterial cell was close yet separated from the bead, and 50–100 pN, when the starting position of the bacterial cell was in direct contact with the bead, were obtained.

Torque generated by flagella rotation in *E. coli* is another interesting application of OT to microorganisms. Bacterial cells containing locomotive-specific appendages such as flagella have been a model system for the measurement of force transduction and the motility of cells. A comprehensive review has been made by Berry & Berg (1997) and, recently, the bacterial rotor has been reported by Reid *et al.* (2006) and Darnton *et al.* (2007).

Apart from bacterial cells, OT have also been applied to a range of fungal cell studies. Wright *et al.* (2007) and Burnham *et al.* (2007) have demonstrated the use of single or holographic OT to generate mechanical stimuli for hyphal tips of single fungal cells. The OT have been used to move and rotate a single fungal cell. They can also trap and move organelles with high refractive index, such as a Woronin body within a hypha of *Neurospora crass*. However, organelles of lower refractive index than their surroundings were repelled by the trap. By making use of this function, the laser was located to the side of such an organelle, Spitzenkorper within the hyphal tip, and

this resulted in the redirection of hyphal tip growth away from the trap. Using an optically trapped 4 μm polystyrene bead as an obstacle on the tip of a leading hypha, the hypha was able to push the bead out of the trap so that the growth force of the leading hypha can be estimated. Another mechanostimulus to growing hyphal tips was applied by a 10 μm bead moving back and forth against the hyphal tip at high speeds (up to 40 μm s^{-1}) and repeatedly hitting a growing tip of a leading hypha tip. By driving three porous beads soaked with chemicals, such as latrunculin-B, the chemicals can be delivered to localized regions of hyphae. These wide ranges of techniques using OT for fungal cells can also be applied to other cells.

4. OPTICAL–MECHANICAL INTERPLAY

Most biological cells are highly deformable compared with other colloidal particles. Hence, the holding force generated from photon scattering in optical trapping could impose a certain force on the cell membranes and consequently cause them to deform. Such a complex optical–mechanical effect has not been studied enough, although it could profoundly influence the cell behaviours. Recently, a few studies have attempted to investigate and model such intricate phenomena for RBCs. Guck *et al.* (2000) calculated the stress distribution generated from two divergent counter-propagating beams around a single cell but the cell deformation was obtained from experimental measurements. Dao *et al.* (2003), Lim *et al.* (2004*a*) and Liu *et al.* (2006) presented numerical simulations, based on mechanical models for two-bead attached RBCs, while Bareil *et al.* (2006) numerically simulated the deformation of RBCs by OS. A model using the concept of Euler buckling instability has been used to capture the essential physics of RBC folding in an optical trap (Ghosh *et al.* 2006).

However, the force exerted on cell membranes which is generated from laser trapping still needs to be further quantified. Recently, the models developed for the calculation of the trapping force have been refined and developed (Mazolli *et al.* 2003; Lock 2004; Mao *et al.* 2007; Bonessi *et al.* 2007) and a computational toolbox is also available (Nieminen *et al.* 2007).

5. PROSPECTS

OT have been widely used for nanomechanical characterization as they have the advantages of non-contact force for cell manipulation, force resolution as accurate as 100 aN and amiability to liquid medium environments. This powerful emerging tool is envisaged in many applications for single cell studies in the coming decades. Three future trends in manipulating single cells which can be envisaged are reported here.

5.1. Enabling techniques for improving the capability of OT

Other techniques, such as rapid detection and position devices, Raman spectroscopy and confocal microscopy, and rapid imaging methods, will be combined with the

OT. Position tracking of spherical particles has been available; however, precise position detection of irregularly shaped objects will be more challenging. This technique can be used to measure the deformation of cells exposed to optical laser beams. Various spectroscopy techniques, such as Raman spectrometry, have been used to detect subtle changes at the molecular level so that the response of cells to mechanical and chemical stimuli can be quantitatively characterized. Fluorescence resonance energy transfer (Huebsch & Mooney 2007), a useful technique to probe the response of biological cells to different biomaterials for tissue engineering, and other techniques could be combined with OT for applications in regenerative medicine. Advanced imaging techniques, such as digital holographic microscopy (Lee & Grier 2007) and multiphoton microscopy (Goksör *et al.* 2004), have been used for cell analysis and in combination with these imaging techniques, more applications of OT for single cells are envisioned for the future.

5.2. OT integrated with lab-on-chip devices

OT are easily integrated with microfluidic devices for single cell manipulation (Monat *et al.* 2008). Single cell cultivation in the microfluidic devices with the aid of optical manipulation will produce homogeneous daughter cells that have a significant impact on cell therapy. How cells respond to neighbouring cells, biomaterials or surfaces, and chemical/mechanical stimuli will be studied in the microfluidic platform integrated with optical traps. Cell sorting in the microfluidic platform has been intensively investigated. High throughput, automated, passive cell sorting will become popular for biologists. The cell sorting throughput efficiency will be improved by introducing multiple optical traps. Recently, both near-field optics using the evanescent waves and holographic techniques have been used for the manipulation of a large number of particles simultaneously. Optically bound arrays (Mellor & Bain 2006) and large-area manipulation using surface plasmon field enhancement (Garces-Chavez *et al.* 2006) have been reported for near-field optics. As holographic traps are already under computer control, it is relatively easy to combine HOTs with pattern recognition to automate particle capture and sorting (Chapin *et al.* 2006).

5.3. Creation of three-dimensional complex architecture by OT

HOTs can create multiple traps with free and independent movement in three dimensions. One or more cell types can be organized into spatially well-defined three-dimensional arrays and functional tissues can be produced. Through advanced computer-controlled algorithms, HOTs can create complex patterns and geometries to match real biological tissues. One of the attractive three-dimensional architectural structures is a stem cell niche that is depicted in figure 4. Stem cells can only be functional to reproduce or self-renew when they reside in such an architectural space. The niche includes the stem cell, niche cell or hub cell, extracellular
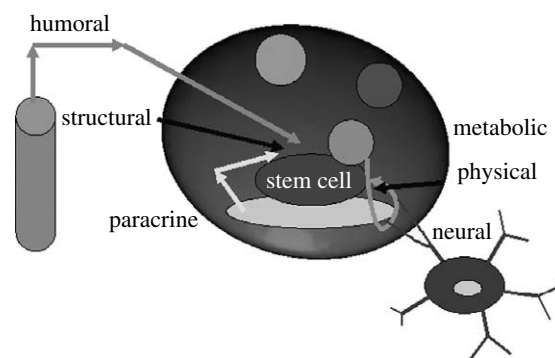

Figure 4. Stem cell niche. Elements are identified for regulating the system of a stem cell, including the constraints of the architectural space, physical engagement of the cell membrane, signalling interactions, neural input and metabolic products of tissue activity. Adapted from Scadden (2006).

matrix and other extracellular components. These elements have to be placed to their anatomic and functional locations and the contact between these elements allows molecular interactions that are crucial for regulating stem cell function (Scadden 2006). HOTs are a potential tool to be employed to accurately place niche cell, stem cell and matrix into the correct sites to create a complex and functional niche. Stem cells cultured in this micromanipulated niche will be developed into functional and sustaining tissues.

REFERENCES

Abbondanzieri, E. A., Greenleaf, W. J., Shaevitz, J. W., Landick, R. & Block, S. M. 2005 Direct observation of base-pair stepping by RNA polymerase. *Nature* **438**, 460–465. (doi:10.1038/nature04268)

Akselrod, G. M., Timp, W., Mirsaidov, U., Zhao, Q., Li, C., Timp, K., Matsudaira, P. & Timp, G. 2006 Laser-guided assembly of heterotypic three-dimensional living cell microarrays. *Biophys. J.* **91**, 3465–3473. (doi:10.1529/biophysj.106.084079)

Allemand, J. F., Bensimon, D. & Croquette, V. 2003 Stretching DNA and RNA to probe their interactions with proteins. *Curr. Opin. Struct. Biol.* **13**, 266–274. (doi:10.1016/S0959-440X(03)00067-8)

Allen, L., Beijersbergen, M. W., Spreeuw, R. J. C. & Woerdman, J. P. 1992 Orbital angular momentum of light and the transformation of laguerre-gaussian laser modes. *Phys. Rev. A* **45**, 8185–8189. (doi:10.1103/PhysRevA.45.8185)

Andersson, M., Madgavkar, A., Stjerndahl, M., Wu, Y., Tan, W., Duran, R., Niehren, S., Mustafa, M. & Arvidson, K. 2007*a* Using optical tweezers for measuring the interaction forces between human bone cells and implant surfaces: system design and force calibration. *Rev. Sci. Instrum.* **78**, 074302. (doi:10.1063/1.2752606)

Andersson, M., Uhlin, B. E. & Fallman, E. 2007*b* The biomechanical properties of *E-coli* pili for urinary tract attachment reflect the host environment. *Biophys. J.* **93**, 3008–3014. (doi:10.1529/biophysj.107.110643)

Applegate, R. W., Squier, J., Vestad, T., Oakey, J. & Marr, D. W. M. 2004 Optical trapping, manipulation, and

sorting of cells and colloids in microfluidic systems with diode laser bars. *Opt. Express* **12**, 4390–4398. (doi:10.1364/OPEX.12.004390)

Applegate, R. W., Squier, J., Vestad, T., Oakey, J., Marr, D. W. M., Bado, P., Dugan, M. A. & Said, A. A. 2006 Microfluidic sorting system based on optical waveguide integration and diode laser bar trapping. *Lab Chip* **6**, 422–426. (doi:10.1039/b512576f)

Asbury, C. L., Fehr, A. N. & Block, S. M. 2003 Kenesin moves by an asymmetric hand-over-hand mechanism. *Science* **302**, 2130–2134. (doi:10.1126/science.1092985)

Ashkin, A. 1970 Acceleration and trapping of particles by radiation pressure. *Phys. Rev. Lett.* **24**, 156–159. (doi:10.1103/PhysRevLett.24.156)

Ashkin, A. 1992 Forces of a single-beam gradient laser trap on a dielectric sphere in the ray optics regime. *Biophys. J.* **61**, 569–582.

Ashkin, A. 1997 Optical trapping and manipulation of neutral particles using lasers. *Proc. Natl Acad. Sci. USA* **94**, 4853–4860. (doi:10.1073/pnas.94.10.4853)

Ashkin, A. 2007 *Optical trapping and manipulation of neutral particles using lasers: a reprint volume with commentaries.* River Edge, NJ: World Scientific.

Ashkin, A. & Dziedzic, J. M. 1987 Optical trapping and manipulation of viruses and bacteria. *Science* **235**, 1517–1520. (doi:10.1126/science.3547653)

Askenasy, N. & Farkas, D. L. 2002 Optical imaging of PKH-labeled hematopoietic cells in recipient bone marrow *in vivo*. *Stem Cells* **20**, 501–513. (doi:10.1634/stemcells.20-6-501)

Ayano, S., Wakamoto, Y., Yamashita, S. & Yasuda, K. 2006 Quantitative measurement of damage caused by 1064-nm wavelength optical trapping of *Escherichia coli* cells using on-chip single cell cultivation system. *Biochem. Biophys. Res. Commun.* **350**, 678–684. (doi:10.1016/j.bbrc.2006.09.115)

Bareil, P. B., Sheng, Y., Chen, Y. Q. & Chiou, A. 2006 Calculation of spherical red blood cell deformation in a dual-beam optical stretcher. *Opt. Express* **15**, 16 029–16 034. (doi:10.1364/OE.15.016029)

Bar-Ziv, R., Moses, E. & Nelson, P. 1998 Dynamic excitations in membranes induced by optical tweezers. *Biophys. J.* **75**, 294–320.

Berg-Sorensen, K. & Flyvbjerg, H. 2004 Power spectrum analysis for optical tweezers. *Rev. Sci. Instrum.* **75**, 594–612. (doi:10.1063/1.1645654)

Berns, M. W. 1998 Laser scissors and tweezers. *Sci. Am.* **278**, 62–67.

Berns, M. W. & Greulich, K. O. 2007 *Laser manipulation of cells and tissues. Methods in cell biology*, vol. 82. New York, NY: Academic Press.

Berns, M. W., Wright, W. H., Tromberg, B. J., Profeta, G. A., Andrews, J. J. & Walter, R. J. 1989 Use of a laser-induced optical force trap to study chromosome movement on the mitotic spindle. *Proc. Natl Acad. Sci. USA* **86**, 4539–4543. (doi:10.1073/pnas.86.12.4539)

Berry, R. M. & Berg, H. C. 1997 Absence of a barrier to backwards rotation of the bacterial flagellar motor demonstrated with optical tweezers. *Proc. Natl Acad. Sci. USA* **94**, 14 433–14 437. (doi:10.1073/pnas.94.26.14433)

Block, S. M., Asbury, C. L., Shaevitz, J. W. & Lang, M. J. 2003 Probing the kinesin reaction cycle with a 2D optical force clamp. *Proc. Natl Acad. Sci. USA* **100**, 2351–2356. (doi:10.1073/pnas.0436709100)

Bonessi, D., Bonin, K. & Walker, T. 2007 Optical forces on particles of arbitrary shape and size. *J. Opt. A* **9**, S228–S234. (doi:10.1088/1464-4258/9/8/S16)

Bronkhorst, P. J. H., Streekstra, G. J., Grimbergen, J., Nijhof, E. J., Sixma, J. J. & Brakenhoff, G. J. 1995 A new method to study shape recovery of red blood cells using multiple optical trapping. *Biophys. J.* **69**, 1666–1673.

Buican, T. N., Smyth, M. J., Crissman, H. A., Salzman, G. C., Stewart, C. C. & Martin, J. C. 1987 Automated single-cell manipulation and sorting by light trapping. *Appl. Opt.* **26**, 5311–5316.

Burnham, D. R., Wright, G. D., Read, N. D. & McGloin, D. 2007 Holographic and single beam optical manipulation of hyphal growth in filamentous fungi. *J. Opt. A* **9**, S172–S179.

Bustamante, C., Bryant, Z. & Smith, S. B. 2003 Ten years of tension: single-molecule DNA mechanics. *Nature* **421**, 423–427. (doi:10.1038/nature01405)

Cecconi, C., Shank, E. A., Bustamante, C. & Marqusee, S. 2005 Direct observation of the three-state folding of a single protein molecule. *Science* **309**, 2057–2060. (doi:10.1126/science.1116702)

Chan, J. W., Taylor, D. S., Zwerdling, T., Lane, S. M., Ihara, K. & Huser, T. 2006 Micro-Raman spectroscopy detects individual neoplastic and normal hematopoietic cells. *Biophys. J.* **90**, 648–652. (doi:10.1529/biophysj.105.066761)

Chapin, S. C., Germain, V. & Dufresne, E. R. 2006 Automated trapping, assembly, and sorting with holographic optical tweezers. *Opt. Express* **14**, 13 095–13 100. (doi:10.1364/OE.14.013095)

Chiou, A. E., Wang, W., Sonek, G. J., Hong, J. & Berns, M. W. 1997 Interferometric optical tweezers. *Opt. Commun.* **133**, 7–10. (doi:10.1016/S0030-4018(96)00456-7)

Cizmar, T., Siler, M., Sery, M., Zemanek, P., Garcés-Chávez, V. & Dholakia, K. 2006 Optical sorting and detection of sub-micron objects in a motional standing wave. *Phys. Rev. B* **74**, 035 105. (doi:10.1103/PhysRevB.74.035105)

Colombelli, J., Grill, S. W. & Stelzer, E. H. K. 2004 Ultraviolet diffraction limited nanosurgery of live biological tissues. *Rev. Sci. Instrum.* **75**, 472–478. (doi:10.1063/1.1641163)

Constable, A., Kim, J., Mervis, J., Zarinetchi, F. & Prentiss, M. 1993 Demonstration of a fibre-optical light-force trap. *Opt. Lett.* **18**, 1867–1869.

Cran-McGreehin, S., Krauss, T. F. & Dholakia, K. 2006 Integrated monolithic optical manipulation. *Lab Chip* **6**, 1122–1124. (doi:10.1039/b605237a)

Creely, C. M., Volpe, G., Singh, G. P., Soler, M. & Petrov, D. V. 2005 Raman imaging of floating cells. *Opt. Express* **13**, 6105–6110. (doi:10.1364/OPEX.13.006105)

Curtis, J. E. & Grier, D. G. 2003 Structure of optical vortices. *Phys. Rev. Lett.* **90**, 133 901. (doi:10.1103/PhysRevLett.90.133901)

Curtis, J. E. & Spatz, J. P. 2004 Getting a grip: hyaluronan-mediated cellular adhesion. *Proc. SPIE* **5514**, 455–466. (doi:10.1117/12.560049)

Curtis, J. E., Koss, B. A. & Grier, D. G. 2002 Dynamic holographic optical tweezers. *Opt. Commun.* **207**, 169–175. (doi:10.1016/S0030-4018(02)01524-9)

Dao, M., Lim, C. T. & Suresh, S. 2003 Mechanics of the human red blood cell deformed by optical tweezers. *J. Mech. Phys. Solids* **51**, 2259–2280. (doi:10.1016/j.jmps.2003.09.019)

Darnton, N. C., Turner, L., Rojevsky, S. & Berg, H. C. 2007 On torque and tumbling in swimming *Escherichia coli*. *J. Bacteriol.* **189**, 1756–1764. (doi:10.1128/JB.01501-06)

Dent, E. W. & Gertler, F. B. 2003 Cytoskeletal dynamics and transport in growth cone motility and axon guidance. *Neuron* **40**, 209–227. (doi:10.1016/S0896-6273(03)00633-0)

Dharmadhikari, J. A., Roy, S., Dharmadhikari, A. K., Sharma, S. & Mathur, D. 2004 Torque-generating malaria-infected red blood cells in an optical trap. *Opt. Express* **12**, 1179–1184. (doi:10.1364/OPEX.12.001179)

Dharmadhikari, J. A., Dharmadhikari, A. K., Makhija, V. S. & Mathur, D. 2007 Multiple optical traps with a single laser beam using a simple and inexpensive mechanical element. *Curr. Sci.* **93**, 1265–1270.

Dholakia, K. & Reece, P. 2006 Optical micromanipulation takes hold. *Nanotoday* **1**, 18–27. (doi:10.1016/S1748-0132(06)70019-6)

Dholakia, K., MacDonald, M. P., Zemanek, P. & Cizmar, T. 2007 Cellular and colloidal separation using optical forces. *Methods Cell Biol.* **82**, 467–495.

Dumont, S., Cheng, W., Serebrov, V., Beran, R. K., Tinoco, I., Pyle, A. M. & Bustamante, C. 2006 RNA translocation and unwinding mechanisms of HCV N53 helicase and its coordination by ATP. *Nature* **439**, 105–110. (doi:10.1038/nature04331)

Durnin, J. 1987 Exact solutions for diffracting beams. I. The scalar theory. *J. Opt. Soc. Am. A* **4**, 651–654.

Ehrlicher, A., Betz, T., Stuhrmann, B., Koch, D., Milner, V., Raizen, M. G. & Kas, J. 2002 Guiding neuronal growth with light. *Proc. Natl Acad. Sci. USA* **27**, 16 024–16 028. (doi:10.1073/pnas.252631899)

Emiliani, V., Cojoc, D., Ferrari, E., Garbin, V., Durieux, C., Coppey-Moisan, M. & Di Fabrizio, E. 2005 Wave front engineering for microscopy of living cells. *Opt. Express* **13**, 1395–1405. (doi:10.1364/OPEX.13.001395)

Enger, J., Goksor, M., Ramser, K., Hagberg, P. & Hanstorp, D. 2004 Optical tweezers applied to a microfluidic system. *Lab Chip* **4**, 196–200. (doi:10.1039/b307960k)

Ericsson, M., Hanstorp, D., Hagberg, P., Enger, J. & Nystrom, T. 2000 Sorting out bacterial viability with optical tweezers. *J. Bacteriol.* **182**, 5551–5555. (doi:10.1128/JB.182.19.5551-5555.2000)

Eriksen, R. L., Daria, V. R. & Glucstad, J. 2002 Fully dynamic multiple-beam optical tweezers. *Opt. Express* **10**, 597–602.

Eriksson, E., Scrimgeour, J., Granéli, A., Ramser, K., Wellander, R., Enger, J. & Goksör, M. 2007 Optical manipulation and microfluidics for studies of single cell dynamics. *J. Opt. A* **9**, S113–S121. (doi:10.1088/1464-4258/9/8/S02)

Fallman, E. & Axner, O. 1997 Design for fully steerable dual-trap optical tweezers. *Appl. Opt.* **36**, 2107–2113.

Fallman, E., Schedin, S., Jass, J., Andersson, M., Uhlin, B. E. & Axner, O. 2004 Optical tweezers based force measurement system for quantitating binding interactions: system design and application for the study of bacterial adhesion. *Biosens. Bioelectron.* **19**, 1429–1437. (doi:10.1016/j.bios.2003.12.029)

Flynn, R. A., Birkbeck, A. L., Gross, M., Ozkan, M., Shao, B., Wang, M. M. & Esener, S. C. 2002 Parallel transport of biological cells using individually addressable VCSEL arrays as optical tweezers. *Sensor. Actuat. B-Chem.* **87**, 239–243. (doi:10.1016/S0925-4005(02)00242-3)

Foo, J. J., Liu, K. K. & Chan, V. 2003 Thermal effect on a viscously deformed liposome in a laser trap. *Ann. Biomed. Eng.* **31**, 354–362. (doi:10.1114/1.1555626)

Foo, J. J., Liu, K. K. & Chan, V. 2004 Viscous drag of deformed vesicles in optical trap: experiments and simulations. *AIChE J.* **50**, 249–254. (doi:10.1002/aic.10023)

Foo, J. J., Chan, V., Feng, Z. Q. & Liu, K. K. 2006 Human red blood cell deformed under thermal fluid flow. *Biomed. Mater.* **1**, 1–7. (doi:10.1088/1748-6041/1/1/001)

Gahagan, K. T. & Swartzlander, G. A. 1998 Trapping of low-index microparticles in an optical vortex. *J. Opt. Soc. Am. B* **15**, 524–534. (doi:10.1364/JOSAB.15.000524)

Gahagan, K. T. & Swartzlander, G. A. 1999 Simultaneous trapping of low-index and high-index microparticles observed with an optical-vortex trap. *J. Opt. Soc. Am. B* **16**, 533–537. (doi:10.1364/JOSAB.16.000533)

Garces-Chavez, V., McGloin, D., Melville, H., Sibbett, W. & Dholakia, K. 2002 Simultaneous micromanipulation in multiple planes using a self-reconstructing light beam. *Nature* **419**, 145–147. (doi:10.1038/nature01007)

Garces-Chavez, V., Quidant, R., Reece, P. J., Badenes, G., Torner, L. & Dholakia, K. 2006 Extended organization of colloidal microparticles by surface plasmon polariton excitation. *Phys. Rev. B* **73**, 085 417. (doi:10.1103/PhysRevB.73.085417)

Ghosh, A., Sinha, S., Dharmadhikari, J. A., Roy, S., Dharmadhikari, A. K., Samuel, J., Sharma, S. & Mathur, D. 2006 Euler buckling-induced folding and rotation of red blood cells in an optical trap. *Phys. Biol.* **3**, 67–73. (doi:10.1088/1478-3975/3/1/007)

Goksör, M., Enger, J. & Hanstorp, D. 2004 Optical manipulation in combination with multiphoton microscopy for single-cell studies. *Appl. Opt.* **43**, 4831–4837. (doi:10.1364/AO.43.004831)

Greenleaf, W. J., Woodside, M. T., Abbondanzieri, E. A. & Block, S. M. 2005 Passive all-optical force clamp for high-resolution laser trapping. *Phys. Rev. Lett.* **95**, 208 102. (doi:10.1103/PhysRevLett.95.208102)

Greenleaf, W. J., Woodside, M. T. & Block, S. M. 2007 High-resolution, single-molecule measurement of biomolecular motion. *Annu. Rev. Biophys. Biomol. Struct.* **36**, 171–190. (doi:10.1146/annurev.biophys.36.101106.101451)

Grier, D. G. 2003 A revolution in optical manipulation. *Nature* **424**, 810–816. (doi:10.1038/nature01935)

Grover, S. C., Gauthier, R. C. & Skirtach, A. G. 2000 Analysis of the behaviour of erythrocytes in an optical trapping system. *Opt. Express* **7**, 533–539.

Grover, S. C., Skirtach, A. G., Gauthier, R. C. & Grover, C. P. 2001 Automated single-cell sorting system based on optical trapping. *J. Biomed. Opt.* **6**, 14–22. (doi:10.1117/1.1333676)

Gu, M., Kuriakose, S. & Gan, X. 2007 A single beam near-field laser trap for optical stretching, folding and rotation of erythrocytes. *Opt. Express* **13**, 1369–1375. (doi:10.1364/OE.15.001369)

Guck, J., Ananthakrishnan, R., Moon, T. J., Cunningham, C. C. & Kas, J. 2000 Optical deformability of soft biological dielectrics. *Phys. Rev. Lett.* **84**, 5451–5454. (doi:10.1103/PhysRevLett.84.5451)

Guck, J., Ananthakrishnan, R., Mahmood, H., Moon, T. J., Cunningham, C. C. & Kas, J. 2001 The optical stretcher: a novel laser tool to micromanipulate cells. *Biophys. J.* **81**, 767–784.

Guck, J., Ananthakrishnan, R., Cunningham, C. C. & Kas, J. 2002 Stretching biological cells with light. *J. Phys. Condens. Matter* **14**, 4843–4856. (doi:10.1088/0953-8984/14/19/311)

Guck, J. *et al.* 2005 Optical deformability as an inherent cell marker for testing malignant transformation and meta-static competence. *Biophys. J.* **88**, 3689–3698. (doi:10.1529/biophysj.104.045476)

Guilford, W. H., Tournas, J. A., Dascalu, D. & Watson, D. S. 2004 Creating multiple time-shared laser traps with simultaneous displacement detection using digital signal processing hardware. *Anal. Biochem.* **326**, 153–166. (doi:10.1016/j.ab.2003.11.025)

Hansen, P. M., Tolic-Norrelykke, I. M., Flyvbjerg, H. & Berg-Sorensen, K. 2006 Tweezercalib 2.0: faster version of

MatLab package for precise calibration of optical tweezers. *Comput. Phys. Commun.* **174**, 518–520. (doi:10.1016/j.cpc.2005.11.007)

Hart, S. J., Terray, A., Leski, T. A., Arnold, J. & Stroud, R. 2006 Discovery of a significant optical chromatographic difference between spores of *Bacillus anthracis* and its close relative, *Bacillus thuringiensis*. *Anal. Chem.* **78**, 3221–3225. (doi:10.1021/ac052221z)

Hart, S. J., Terray, A., Arnold, J. & Leski, T. A. 2007 Sample concentration using optical chromatography. *Opt. Express* **15**, 2724–2731. (doi:10.1364/OE.15.002724)

He, H., Friese, M. E. J., Heckenberg, N. R. & Rubinsztein-Dunlop, H. 1995 Direct observation of transfer of angular momentum to absorptive particles from a laser beam with a phase singularity. *Phys. Rev. Lett.* **75**, 826–829. (doi:10.1103/PhysRevLett.75.826)

Henon, S., Lenormand, G., Richert, A. & Gallet, F. 1999 A new determination of the shear modulus of the human erythrocyte membrane using optical tweezers. *Biophys. J.* **76**, 1145–1151.

Herzenberg, L. A., Parks, D., Sahaf, B., Perez, O., Roederer, M. & Herzenberg, L. A. 2002 The history and future of the fluorescence activated cell sorter and flow cytometry: a view from Stanford. *Clin. Chem.* **48**, 1819–1827.

Hoffmann, A., Horste, G. M. Z., Pilarczyk, G., Monajembashi, S., Uhl, V. & Greulich, K. O. 2000 Optical tweezers for confocal microscopy. *Appl. Phys. B* **71**, 747–753. (doi:10.1007/s003400000454)

Hormeno, S. & Arias-Gonzalez, J. R. 2006 Exploring mechanchemical processes in the cell with optical tweezers. *Biol. Cell.* **98**, 679–695. (doi:10.1042/BC20060036)

Huang, W., Anvari, B., Torres, J. H., LeBaron, R. G. & Athanasiou, K. A. 2003 Temporal effects of cell adension on mechanical characteristics of the single chondrocyte. *J. Orthopaed. Res.* **21**, 88–95. (doi:10.1016/S0736-0266(02)00130-4)

Huebsch, N. D. & Mooney, D. J. 2007 Fluorescent resonance energy transfer: a tool for probing molecular cell–biomaterial interactions in three dimensions. *Biomaterials* **28**, 2424–2437. (doi:10.1016/j.biomaterials.2007.01.023)

Huisstede, J. H. G., Subramaniam, V. & Bennink, M. L. 2007 Combining optical tweezers and scanning probe microscopy to study DNA–protein interactions. *Microsc. Res. Tech.* **70**, 26–33. (doi:10.1002/jemt.20382)

Ichikawa, M. & Yoshikawa, K. 2001 Optical transport of a single cell-sized lipsome. *Appl. Phys. Lett.* **79**, 4598–4600. (doi:10.1063/1.1430026)

Imasaka, T., Kawabata, Y., Kaneta, T. & Ishidzu, Y. 1995 Optical chromatography. *Anal. Chem.* **67**, 1763–1765. (doi:10.1021/ac00107a003)

Jass, J., Schedin, S., Fallman, E., Ohlsson, J., Nilsson, U. J., Uhlin, B. E. & Axner, O. 2004 Physical properties of *Escherichia coli* P pili measured by optical tweezers. *Biophys. J.* **87**, 4271–4283. (doi:10.1529/biophysj.104.044867)

Jauffred, L., Callisen, T. H. & Oddershede, L. B. 2007 Viscoelastic membrane tethers extracted from *Escherichia coli* by optical tweezers. *Biophys. J.* **93**, 4068–4075. (doi:10.1529/biophysj.107.103861)

Jess, P. R. T., Garces-Chavez, V., Smith, D., Mazilu, M., Paterson, L., Riches, A., Herrington, C. S., Sibbett, W. & Dholakia, K. 2006 Dual beam fibre trap for Raman microspectroscopy of single cells. *Opt. Express* **14**, 5779–5791. (doi:10.1364/OE.14.005779)

Jordan, P. *et al.* 2005 Creating permanent 3D arrangements of isolated cells using holograhpic optical tweezers. *Lab Chip* **5**, 1224–1228. (doi:10.1039/b509218c)

Kaneta, T., Ishidzu, Y., Mishima, N. & Imasaka, T. 1997 Theory of optical chromatography. *Anal. Chem.* **69**, 2701–2710. (doi:10.1021/ac970079z)

Keen, S., Leach, J., Gibson, G. & Padgett, M. J. 2007 Comparison of a high-speed camera and a quadrant detector for measuring displacements in optical tweezers. *J. Opt. A: Pure Appl. Opt.* **9**, S264–S266. (doi:10.1088/1464-4258/9/8/S21)

Knight, A. E., Veigel, C., Chambers, C. & Molloy, J. E. 2001 Analysis of single-molecule mechanical recordings: application to acto-myosin interactions. *Prog. Biophys. Mol. Biol.* **77**, 45–72. (doi:10.1016/S0079-6107(01)00010-4)

Knoner, G., Rolfe, B. E., Campbell, J. H., Parkin, S. J., Heckenberg, N. R. & Rubinsztein-Dunlop, H. 2006 Mechanics of cellular adhesion to artificial artery templates. *Biophys. J.* **91**, 3085–3096. (doi:10.1529/biophysj.105.076125)

Konig, K., Liang, H., Berns, M. W. & Tromberg, B. J. 1996*a* Cell damage in near-infrared multimode optical traps as a result of multiphoton absorption. *Opt. Lett.* **21**, 1090–1092.

Konig, K., Tadir, Y., Patrizio, P., Berns, M. W. & Tromberg, B. J. 1996*b* Effects of ultraviolet exposure and near-infrared laser tweezers on human spermatozoa. *Hum. Reprod.* **11**, 2162–2164.

Kumar, S., Maxwell, I. Z., Heisterkamp, A., Polte, T. R., Lele, T. P., Salanga, M., Mazur, E. & Ingber, D. E. 2006 Viscoelastic retraction of single living stress fibers and its impact on cell shape, cytoskeletal organization, and extracellular matrix mechanics. *Biophys. J.* **90**, 3762–3773. (doi:10.1529/biophysj.105.071506)

Ladavac, K., Kasza, K. & Grier, D. G. 2004 Sorting mesoscopic objects with periodic potential landscapes: optical fractionation. *Phys. Rev. E* **70**, 010 901. (doi:10.1103/PhysRevE.70.010901)

Leach, J., Sinclair, G., Jordan, P., Courtial, J., Padgett, M. J., Cooper, J. & Laczik, Z. J. 2004 3D manipulation of particles into crystal structures using holographic optical tweezers. *Opt. Express* **12**, 220–226. (doi:10.1364/OPEX.12.000220)

Lee, S. H. & Grier, D. G. 2007 Holographic microscopy of holographically trapped three-dimensional structures. *Opt. Express* **15**, 1505–1512. (doi:10.1364/OE.15.001505)

Leitz, G., Fallman, E., Tuck, S. & Axner, O. 2002 Stress response in *Caenorhabditis elegans* caused by optical tweezers: wavelength, power, and time dependence. *Biophys. J.* **82**, 2224–2231.

Leitz, G., Lundberg, C., Fallman, E., Axner, O. & Sellstedt, A. 2003 Laser-based micromanipulation for separation and identification of individual Frankia vesicles. *FEMS Microbiol. Lett.* **224**, 97–100. (doi:10.1016/S0378-1097(03)00435-X)

Lenormand, G., Henon, S., Richert, A., Simeon, J. & Gallet, F. 2001 Direct measurement of the area expansion and shear moduli of the human red blood cell membrane skeleton. *Biophys. J.* **81**, 43–56.

Li, Z., Anvari, B., Takashima, M., Brecht, P., Torres, J. H. & Brownell, W. E. 2002 Membrane tether formation from outer hair cells with optical tweezers. *Biophys. J.* **82**, 1386–1395.

Li, C., Liu, Y. P., Liu, K. K. & Lai, A. C. K. 2006 The deformation of an erythrocyte under the radiation pressure by optical stretch. *J. Biomech. Eng., ASME* **128**, 830–836. (doi:10.1115/1.2354204)

Liang, H., Vu, K. T., Krishnan, P., Trang, T. C., Shin, D., Kimel, S. & Berns, M. W. 1996 Wavelength dependence of cell cloning efficiency after optical trapping. *Biophys. J.* **70**, 1529–1533.

Liang, M. N., Smith, S. P., Metallo, S. J., Choi, I. S., Prentiss, M. & Whitesides, G. M. 2000 Measuring the forces

involved in polyvalent adhesion of uropathogenic *Escherichia coli* to mannose-presenting surfaces. *Proc. Natl Acad. Sci. USA* **97**, 13 092–13 096. (doi:10.1073/pnas. 230451697)

Libal, A., Reichhardt, C., Janko, B. & Reichhardt, C. J. O. 2006 Dynamics, rectification, and fractionation for colloids on flashing substrates. *Phys. Rev. Lett.* **96**, 188 301. (doi:10.1103/PhysRevLett.96.188301)

Lim, C. T., Dao, M., Suresh, S., Sow, C. H. & Chew, K. T. 2004a Large deformation of living cells using laser traps. *Acta Mater.* **52**, 1837–1845. (doi:10.1016/j.actamat.2003. 12.028)

Lim, C. T., Dao, M., Suresh, S., Sow, C. H. & Chew, K. T. 2004b Corrigendum to "Large deformation of living cells using laser traps". *Acta Mater.* **52**, 4065–4066. (doi:10. 1016/j.actamat.2004.05.016)

Litvinov, R. I., Bennett, J. S., Weisel, J. W. & Shuman, H. 2005 Multi-step fibrinogen binding to the integrin αIIbβ3 detected using force spectroscopy. *Biophys. J.* **89**, 2824–2834. (doi:10.1529/biophysj.105.061887)

Liu, Y., Cheng, D. K., Sonek, G. J., Berns, M. W., Chapman, C. F. & Tromberg, B. J. 1995 Evidence for localized cell heating induced by infrared optical tweezers. *Biophys. J.* **68**, 2137–2144.

Liu, Y., Sonek, G. J., Berns, M. W. & Tromberg, B. J. 1996 Physiological monitoring of optically trapped cells: assessing the effects of confinement by 1064-nm laser tweezers using microfluorometry. *Biophys. J.* **71**, 2158–2167.

Liu, Y. P., Li, C. & Lai, A. C. K. 2006 Experimental study on the deformation of erythrocytes under optically trapping and stretching. *Mater. Sci. Eng. A* **423**, 128–133. (doi:10. 1016/j.msea.2005.10.077)

Lock, J. A. 2004 Calculation of the radiation trapping force for laser tweezers by use of generalized Lorenz–Mie theory. II. On-axis trapping force. *Appl. Opt.* **43**, 2545–2554. (doi:10.1364/AO.43.002545)

Lucio, A. D., Santos, R. A. S. & Mesquita, O. N. 2003 Measurement and modeling of water transport and osmoregulation in a single kidney cell using optical tweezers and videomicroscopy. *Phys. Rev. E* **68**, 041906. (doi:10.1103/PhysRevE.68.041906)

MacDonald, M. P., Spalding, G. C. & Dholakia, K. 2003 Microfluidic sorting in an optical lattice. *Nature* **426**, 421–424. (doi:10.1038/nature02144)

MacDonald, M. P., Neale, S., Paterson, L., Riches, A., Dholakia, K. & Spalding, G. C. 2004 Cell cytometry with a light touch: sorting microscopic matter with an optical lattice. *J. Biol. Regul. Homeost. Agents* **18**, 200–205.

Maier, B. 2005 Using laser tweezers to measure twitching motility in Neisseria. *Curr. Opin. Microbiol.* **8**, 344–349. (doi:10.1016/j.mib.2005.04.002)

Maier, B., Koomey, M. & Sheetz, M. P. 2004 A force-dependent switch reverses type IV pilus retraction. *Proc. Natl Acad. Sci. USA* **101**, 10 961–10 966. (doi:10.1073/ pnas.0402305101)

Mallik, R., Carter, B. C., Lex, S. A., King, S. J. & Gross, S. P. 2004 Cytoplasmic dynein functions as a gear in response to load. *Nature* **427**, 649–652. (doi:10.1038/nature02293)

Mao, F. L., Xing, Q. R., Wang, K., Lang, L. Y., Chai, L. & Wang, Q. Y. 2007 Calculation of axial optical forces exerted on medium-sized particles by optical trap. *Opt. Laser Technol.* **39**, 34–39. (doi:10.1016/j.optlastec.2005. 05.013)

Martin-Badosa, E., Montes-Usategui, M., Carnicer, A., Andilla, J., Pleguezuelos, E. & Juvells, I. 2007 Design strategies for optimizing holographic optial tweezers setups. *J. Opt. A* **9**, S267–S277.

Mazolli, A., Neto, P. A. M. & Nussenzveig, H. M. 2003 Theory of trapping forces in optical tweezers. *Proc. R. Soc. A* **459**, 3021–3041. (doi:10.1098/rspa.2003.1164)

Mellor, C. D. & Bain, C. D. 2006 Array formation in evanescent waves. *Chem. Phys. Chem.* **7**, 329–332.

Milne, G., Rhodes, D., MacDonald, M. & Dholakia, K. 2007 Fractionation of polydisperse colloid with acousto-optically generated potential energy landscapes. *Opt. Lett.* **32**, 1144–1146. (doi:10.1364/OL.32.001144)

Mohanty, S. K., Uppal, A. & Gupta, P. K. 2004 Self-rotation of red blood cells in optical tweezers: prospects for high throughput malaria diagnosis. *Biotech. Lett.* **26**, 971–974. (doi:10.1023/B:BILE.0000030041.94322.71)

Mohanty, S. K., Dasgupta, R. & Gupta, P. K. 2005a Three-dimensional orientation of microscopic objects using combined elliptical and point optical tweezers. *Appl. Phys. B* **81**, 1063–1066. (doi:10.1007/s00340-005-1970-7)

Mohanty, S. K., Sharma, M., Panicker, M. M. & Gupta, P. K. 2005b Controlled induction, enhancement, and guidance of neuronal growth cones by use of line optical tweezers. *Opt. Lett.* **30**, 2596–2598. (doi:10.1364/OL.30.002596)

Monat, C. *et al.* 2008 Optofluidics: a novel generation of reconfigurable and adaptive compact architectures. *Microfluid. Nanofluid.* **4**, 81–95. (doi:10.1007/s10404-007-0222-z)

Nascimento, J. L., Botvinick, E. L., Shi, L. Z., Durrant, B. & Berns, M. W. 2006 Analysis of sperm motility using optical tweezers. *J. Biomed. Opt.* **11**, 044 001. (doi:10.1117/ 1.2337559)

Neuman, K. C. & Block, S. M. 2004 Optical trapping. *Rev. Sci. Instrum.* **75**, 2787–2809. (doi:10.1063/1.1785844)

Neuman, K. C., Chadd, E. H., Liou, G. F., Bergman, K. & Block, S. M. 1999 Characterization of photodamage to *Escherichia coli* in optical traps. *Biophys. J.* **77**, 2856–2863.

Nieminen, T. A., Loke, V. L. Y., Stilgoe, A. B., Knöner, G., Brańczyk, A. M., Heckenberg, N. R. & Rubinsztein-Dunlop, H. 2007 Optical tweezers computational toolbox. *J. Opt. A* **9**, S196–S203. (doi:10.1088/1464-4258/9/8/S12)

Oakey, J., Allely, J. & Marr, D. W. M. 2002 Laminar-flow-based separations at the microscale. *Biotechnol. Prog.* **18**, 1439–1442. (doi:10.1021/bp0256216)

Oheim, M. & Schapper, F. 2005 Non-linear evanescent-field imaging. *J. Phys. D Appl. Phys.* **38**, R185–R197. (doi:10. 1088/0022-3727/38/10/R01)

Ozkan, M., Pisanic, T., Scheel, J., Barlow, C., Esener, S. & Bhatia, S. N. 2003a Electro-optical platform for the manipulation of live cells. *Langmuir* **19**, 1532–1538. (doi:10.1021/la0261848)

Ozkan, M., Wang, M., Ozkan, C., Flynn, R., Birkbeck, A. & Esener, S. 2003b Optical manipulation of objects and biological cells in microfluidic devices. *Biomed. Micro-devices* **5**, 61–67. (doi:10.1023/A:1024467417471)

Paterson, L. *et al.* 2005 Light-induced cell separation in a tailored optical landscape. *Appl. Phys. Lett.* **87**, 123 901. (doi:10.1063/1.2045548)

Pease, P. J., Levy, O., Cost, G. J., Gore, J., Ptacin, J. L., Sherratt, D., Bustamante, C. & Cozzarelli, N. R. 2005 Sequence-directed DNA transcription by purified FtsK. *Science* **307**, 586–590. (doi:10.1126/science.1104885)

Peterman, E. J. G., Gittes, F. & Schmidt, C. F. 2003 Laser-induced heating in optical traps. *Biophys. J.* **84**, 1308–1316.

Ramser, K., Enger, J., Goksor, M., Hanstorp, D., Logg, K. & Kall, M. 2005 A microfluidic system enabling Raman measurements of the oxygenation cycle in single optically trapped red blood cells. *Lab Chip* **5**, 431–436. (doi:10.1039/ b416749j)

Reid, S. W., Leake, M. C., Chandler, J. H., Lo, C. J., Armitage, J. P. & Berry, R. M. 2006 The maximum number of torque-generating units in the flagellar motor of *Escherichia coli* is at least 11. *Proc. Natl Acad. Sci. USA* **103**, 8066–8071. (doi:10.1073/pnas.0509932103)

Ricardez-Vargas, I., Rodriguez-Montero, P., Ramos-Garcia, R. & Volke-Sepulveda, K. 2006 Modulated optical sieve for sorting of polydisperse microparticles. *Appl. Phys. Lett.* **88**, 121116. (doi:10.1063/1.2183357)

Rodrigo, P. J., Eriksen, R. L., Daria, V. R. & Gluckstad, J. 2003 Shack–Hartmann multiple-beam optical tweezers. *Opt. Express* **11**, 208–214.

Rodrigo, P. J., Perch-Nielsen, I. R. & Gluckstad, J. 2006 Three-dimensional forces in gpc-based counterpropagating-beam traps. *Opt. Express* **14**, 5812–5822. (doi:10.1364/OE.14.005812)

Rohrbach, A. 2005 Switching and measuring a force of 25 femtonewtons with an optical trap. *Opt. Express* **13**, 9695–9701. (doi:10.1364/OPEX.13.009695)

Ryu, W. S., Berry, R. M. & Berg, H. C. 2000 Torque-generating units of the flagellar motor of *Escherichia coli* have a high duty ratio. *Nature* **403**, 444–447. (doi:10.1038/35000233)

Scadden, D. T. 2006 The stem-cell niche as an entity of action. *Nature* **441**, 1075–1079. (doi:10.1038/nature04957)

Schonbrun, E., Piestun, R., Jordan, P., Cooper, J., Wulff, K. D., Courtial, J. & Padgett, M. 2005 3D interferometric optical tweezers using a single spatial light modulator. *Opt. Express* **13**, 3777–3786. (doi:10.1364/OPEX.13.003777)

Schopper, B., Ludwig, M., Edenfeld, J., Al-Hasani, S. & Diedrich, K. 1999 Possible applications of lasers in assisted reproductive technologies. *Hum. Reprod.* **14**(Suppl. 1), 186–193.

Shao, B., Shi, L. Z., Nascimento, J. M., Botvinick, E. L., Ozkan, M., Berns, M. W. & Esener, S. C. 2007 High-throughput sorting and analysis of human sperm with a ring-shaped laser trap. *Biomed. Microdevices* **9**, 361–369. (doi:10.1007/s10544-006-9041-3)

Sheetz, M. P. 1998 *Laser tweezers in cell biology. Methods in cell biology*, vol. 55. New York, NY: Academic Press.

Shi, L. Z., Nascimento, J., Chandsawangbhuwana, C., Berns, M. W. & Botvinick, E. L. 2006 Real-time automated tracking and trapping system for sperm. *Microsc. Res. Tech.* **69**, 894–902. (doi:10.1002/jemt.20359)

Singh, G. P., Creely, C., Volpe, G., Groetsch, H. & Petrov, D. V. 2005 Real-time detection of hyperosmotic stress response in optically trapped single yeast cells using Raman microspectroscopy. *Anal. Chem.* **77**, 2564–2568. (doi:10.1021/ac048359j)

Sleep, J., Wilson, D., Parker, K., Winlove, C. P., Simmons, R. & Gratzer, W. 1999 Elastic properties of the red blood cell membrane measured using optical tweezers: relation to haemolytic disorders. *Biophys. J.* **77**, 3085–3095.

Smith, R. L., Spalding, G. C., Dholakia, K. & MacDonald, M. P. 2007 Colloidal sorting in dynamic optical lattices. *J. Opt. A* **9**, S134–S138.

Steubing, R. W., Cheng, S., Wright, W. H., Numajiri, Y. & Berns, M. W. 1991 Laser induced cell fusion in combination with optical tweezers: the laser cell fusion trap. *Cytometry* **12**, 505–510. (doi:10.1002/cyto.990120607)

Stevenson, D. J., Lake, T. K., Agate, B., Garces-Chavez, V., Dholakia, K. & Gunn-Moore, F. 2006 Optically guided neuronal growth at near infrared wavelengths. *Opt. Express* **14**, 9786–9793. (doi:10.1364/OE.14.009786)

Stuhrmann, B., Jahnke, H. G., Schmidt, M., Hahn, K., Betz, T., Muller, K., Rothemel, A., Kas, J. & Robitzki,

A. A. 2006 Versatile optical manipulation system for inspection, laser processing, and isolation of individual living cells. *Rev. Sci. Instrum.* **77**, 063 116. (doi:10.1063/1.2214961)

Suresh, S., Spatz, J., Mills, J. P., Micoulet, A., Dao, M., Lim, C. T., Beil, M. & Sefferlein, T. 2005 Connections between single-cell biomechanics and human disease states: gastrointestinal cancer and malaria. *Acta Mater.* **1**, 16–30.

Svoboda, K. & Block, S. M. 1994 Biological applications of optical forces. *Ann. Rev. Biophys. Struct.* **23**, 247–285. (doi:10.1146/annurev.bb.23.060194.001335)

Swank, D. M., Bartoo, M. L., Knowles, A. F., Iliffe, C., Bernstein, S. I., Molloy, J. E. & Sparrow, J. C. 2001 Alternative exon-encoded regions of Droscophila myosin heavy chain modulate ATPase rates and actin sliding velocity. *J. Biol. Chem.* **276**, 15 117–15 124. (doi:10.1074/jbc.M008379200)

Terray, A., Arnold, J. & Hart, S. J. 2005 Enhanced optical chromatography in a PDMS microfluidic system. *Opt. Express* **13**, 10 406–10 415. (doi:10.1364/OPEX.13.010406)

Thoumine, O., Kocian, P., Kottelat, A. & Meister, J. J. 2000 Short-term binding of fibroblasts to fibronectin: optical tweezers experiments and probabilistic analysis. *Eur. Biophys. J.* **29**, 398–408. (doi:10.1007/s002490000087)

Titushkin, I. & Cho, M. 2006 Distinct membrane mechanical properties of human mesenchymal stem cells determined using laser optical tweezers. *Biophys. J.* **90**, 2582–2591. (doi:10.1529/biophysj.105.073775)

Townes-Anderson, E., Jules, R. S. S. T., Sherry, D. M., Lichtenberger, J. & Hassanain, M. 1998 Micromanipulation of retinal neurons by optical tweezers. *Mol. Vis.* **4**, 12.

Viana, N. B., Rocha, M. S., Mesquita, O. N., Mazolli, A., Neto, P. A. M. & Nussenzveig, H. M. 2007 Towards absolute calibration of optical tweezers. *Phys. Rev. E* **75**, 021 914. (doi:10.1103/PhysRevE.75.021914)

Visscher, K., Brakenhoff, G. J. & Krol, J. J. 1993 Micromanipulation by multiple optical traps created by a single fast scanning trap integrated with the bilateral confocal scanning laser microscope. *Cytometry* **14**, 105–114. (doi:10.1002/cyto.990140202)

Vossen, D. L. J., van der Horst, A., Dogterom, M. & van Blaaderen, A. 2004 Optical tweezers and confocal microscopy for simultaneous three-dimensional manipulation and imaging in concentrated colloidal dispersions. *Rev. Sci. Instrum.* **75**, 2960–2970. (doi:10.1063/1.1784559)

Wakamoto, Y., Inoue, I., Moriguchi, H. & Yasuda, K. 2001 Analysis of single-cell differences by use of an on-chip microculture system and optical trapping. *Fresen. J. Anal. Chem.* **371**, 276–281. (doi:10.1007/s002160100999)

Walker, L. M., Holm, A., Cooling, L., Maxwell, L., Oberg, A., Sundqvist, T. & El Haj, A. J. 1999 Mechanical manipulation of bone and cartilage cells with 'optical tweezers'. *FEBS Lett.* **459**, 39–42. (doi:10.1016/S0014-5793(99)01169-2)

Watson, D., Hagen, N., Diver, J., Marchand, P. & Chachisvilis, M. 2004 Elastic light scattering from single cells: orientational dynamics in optical trap. *Biophys. J.* **87**, 1298–1306. (doi:10.1529/biophysj.104.042135)

Wang, M. M. *et al.* 2005 Microfluidic sorting of mammalian cells by optical force switching. *Nat. Biotech.* **23**, 83–87. (doi:10.1038/nbt1050)

Waugh, R. & Evans, E. A. 1979 Thermoelasticity of red blood cell membrane. *Biophys. J.* **26**, 115–132.

Williams, M. C., Rouzina, I., Wenner, J. R., Gorelick, R. J., Musier-Forsyth, K. & Bloomfield, V. A. 2001 Mechanism for nucleic acid chaperone activity of HIV-1 nucleocapsid

protein revealed by single molecule stretching. *Proc. Natl Acad. Sci. USA* **98**, 6121–6126. (doi:10.1073/pnas. 101033198)

Wright, G. D., Arlt, J., Poon, W. C. K. & Read, N. D. 2007 Optical tweezer micromanipulation of filamentous fungi. *Fungal Gene. Biol.* **44**, 1–13. (doi:10.1016/j.fgb.2006.07.002)

Xie, C. G., Dinno, M. A. & Li, Y. Q. 2002 Near-infrared Raman spectroscopy of single optically trapped biological cells. *Opt. Lett.* **27**, 249–251. (doi:10.1364/OL.27.000249)

Xie, C., Mace, J., Dinno, M. A., Li, Y. Q., Tang, W., Newton, R. J. & Gemperline, P. J. 2005 Identification of single bacterial cells in aqueous solution using conflocal laser tweezers Raman spectroscopy. *Anal. Chem.* **77**, 4390–4397. (doi:10.1021/ac0504971)

Zemanek, P., Karasek, V. & Sery, M. 2004 Behaviour of colloidal microparticles in a planar 3-beam interference field. *Proc. SPIE* **5514**, 15–26. (doi:10. 1117/12.557183)

Zheng, F., Qin, Y. & Chen, K. 2007 Sensitivity map of laser tweezers Raman spectroscopy for single-cell analysis of colorectal cancer. *J. Biomed. Opt.* **12**, 034 002. (doi:10. 1117/1.2748060)